

MINERALOGICAL COMPOSITION AND PARTICLE SIZE DISTRIBUTION
OF THE HARMATTAN DUST HAZE

By

ABUBAKAR GANI AHMED

Submitted to the Postgraduate School, Ahmadu Bello
University, in Partial Fulfilment of the Requirements
for the Degree of MASTER OF SCIENCE (PHYSICS).

DEPARTMENT OF PHYSICS
AHMADU BELLO UNIVERSITY, ZARIA

DECLARATION

The work reported in this thesis has been carried out by the author under the supervision of Dr. J. Adetunji. It has not been accepted elsewhere for the award of higher degree or diploma. The works of other investigators are acknowledged and referred to accordingly.



A. G. AHMED
(Author)
Department of Physics
Ahmadu Bello University
ZARIA

5 - 1 - 1987

DATE

CERTIFICATION

This thesis entitled MINERALOGICAL COMPOSITION AND PARTICLE SIZE DISTRIBUTION OF THE HARMATTAN DUST HAZE by Mr. Abubakar Gani AHMED, meets the regulations governing the award of the degree of Master of Science, Physics of Ahmadu Bello University, Zaria, and is approved for its contribution to knowledge and literary presentation.



DR. J. ADETUNJI
Chairman, Supervisory Committee
and Head, Physics Department
Ahmadu Bello University
ZARIA

10th January 1987
.....
Date



DR. E.T. MICAH
Member, Supervisory Committee
Physics Department
Ahmadu Bello University
ZARIA

10/1/87
.....
Date

Professor G.E. Osuidi
Dean, Postgraduate School
Ahmadu Bello University
ZARIA

.....
Date

DEDICATION

To my Mother

ACKNOWLEDGEMENTS

Thanks be to Allah who has provided me with the ability to go so far in the pursuit of knowledge for the benefit of mankind.

Much thanks and sincere gratitude go to my Supervisor, Dr. J. Adetunji for his help, guidance and understanding throughout this work. Infact the personal interest he has shown in this work was my main driving force. The constructive criticisms and suggestions offered by Dr. E.T. Micah, the co-supervisor of this project are fully appreciated and acknowledged. I am also grateful to the Department of Physics and Centre for Energy Research and Training, Ahmadu Bello University, Zaria for allowing me to use their facilities, to the Weather Office of Institute of Agricultural Research for supplying the meteorological data. The useful assistance and suggestions rendered by the following staff members of Physics Department are acknowledged. They are Mr. D.D. Afuwai who has been of great help whenever there is a problem with the analytical instruments and he has always proved to be equal to the task, Mr. Bamgbelu, Owobu, Adzua, Fagbemi. I thank Godwin Awah who typed the manuscript. I wish to acknowledge suggestions on data analysis given by Dr. Dorvlo of Mathematics Department and on photography by Malam Baba and Samuel of Geology Department respectively.

Moral and friendly support were received from the following: H.B. Garba, U.F. Bako, Umar Attahir, Abubakar Kaoje, M.B. Danjaji, Adamu Kutigi, L.H. Gusau, Chika Malami,

Ahmed Y. Dadah, Sani Dangoggo, A'isha, L.M.G. and others too numerous to mention here. Their contributions in one way or the other in making this work a success are fully appreciated.

I would also like to thank the University of Sokoto for providing the fellowship for this work, and members of staff of Physics Department, University of Sokoto who shouldered the extra workload caused by my absence.

Finally, to my parents, brothers, sister and other relations whose love and affection has always been my source of inspiration.

ABSTRACT

Harmattan dust collected in Zaria 11°N, 7°38'E, Nigeria, with a four stage Casella MK 2a Cascade impactor was subjected to qualitative x-ray, optical and electron microscopy analyses. Counting and sizing were done with a TGZ-3 counter and Porton graticule.

The results of the x-ray analysis show that the dust consists of Quartz (SiO_2), Microcline ($\text{KA}_1\text{Si}_3\text{O}_8$) which until this time has not been reported to be present in the Harmattan dust, and small concentrations of other clay minerals. It was also observed that:

- (a) the mineralogical composition and shape factors of the dust particles are size range dependent,
- (b) the analysis of particle size measurements gave a log-normal distribution with a mean diameter of 1.03 μm and a geometric standard deviation of 2.33,
- (c) the particle counting and sizing depends on the type of counter used,
- (d) the number-size distribution is independent of the type of microscope used.

TABLE OF CONTENTS

| <u>Chapter</u> | | <u>Page</u> |
|----------------|---|-------------|
| | Title Page | i |
| | Declaration | ii |
| | Certification | iii |
| | Dedication | iv |
| | Acknowledgements | v |
| | Abstract | vii |
| | Table of Contents | viii |
| | List of Tables | x |
| | List of Figures | xi |
| | List of Appendices | xii |
| 1. | INTRODUCTION | 1 |
| 1.1 | Generation of Harmattan Dust | 1 |
| 1.2 | Possible Effects of Harmattan Dust Haze .. | 4 |
| 1.2.1 | Environmental Effects | 4 |
| 1.2.2 | Climatic effects | 5 |
| 1.2.3 | Health effects | 5 |
| 1.3 | A Review of Previous Work on Saharan Dust | 6 |
| 1.4 | Particle Size Distribution | 7 |
| 2. | GENERAL THEORY AND SOURCE OF ERROR IN AEROSOL SAMPLING | 14 |
| 2.1 | Introduction | 14 |
| 2.2 | Instrumentation | 16 |
| 2.3 | Sampling | 16 |
| 3. | QUALITATIVE X-RAY ANALYSIS | 21 |
| 3.1 | Sample Preparation | 21 |
| 3.2 | Procedure of Identification of Minerals | 21 |

| | | |
|-------|--|----|
| 4. | EXPERIMENTAL TECHNIQUES FOR SIZE DISTRIBUTION MEASUREMENTS | 25 |
| 4.1. | Analysis with the Light Microscope ;... | 25 |
| 4.1.1 | Counting and sizing of dust particles | 25 |
| 4.1.2 | Determination of shape factors | 26 |
| 4.2 | Analysis with the Transmission Electron Microscope | 28 |
| 4.2.1 | Specimen preparation | 29 |
| 5. | RESULTS OF PARTICLE SIZE MEASUREMENT | 33 |
| 5.1 | Optical Microscopy Results | 33 |
| 5.1.1 | Calculation of shape factors | 43 |
| 5.2 | Transmission Electron Microscopy Results | 46 |
| 6. | DISCUSSION, CONCLUSION AND SUGGESTION FOR FURTHER WORK | 52 |
| 6.1 | Discussion | 52 |
| 6.2 | Conclusion and Suggestion for Further Work | 57 |
| | REFERENCES | 60 |
| | APPENDIX A | 67 |

LIST OF TABLES

| <u>Table</u> | <u>Title</u> | <u>Page</u> |
|--------------|---|-------------|
| 1. | Calculated values of an-isokinetic effect of the Cascade Impactor | 16 |
| 2. | Mass of the Samples collected and the period of Collection | 19 |
| 3. | Mineral Composition of the Farnattan dust on each stage | 24 |
| 4. | Value of mean diameter (\bar{D}) in microns for each of the four stages of the impactor | 39 |
| 5. | Surface area and volume shape factors for each of the four stages of the impactor | 46 |
| 6. | Mean diameter (\bar{D}) in microns using optical and transmission electron microscope | 48 |
| 7. | Comparison between optical and electron microscope counts of stage 3 and 4 | 50 |

LIST OF FIGURES

| <u>Figure</u> | <u>Title</u> | <u>Page</u> |
|---------------|---|-------------|
| 1. | Trajectories of Harmattan dust Haze | 2 |
| 2. | Three different types of diamters assigned to particles in different orientations... | 9 |
| 3. | Arrangement of the Sample Collector on top of Department of Physics laboratory building | 17 |
| 4. | X-ray diffraction traces of the Sample collected on the four stages of Cascade Impactor | 23 |
| 5. | A metal jig for collecting film on the grids placed on the six holes | 30 |
| 6. | Arrangement used for evaluating the thickness of coating | 32 |
| 7. | Photomicrographs of the particles collected on each of the four stages. Stage 1(a), Stage 2(b), Stage 3(c), Stage 4(d) | 34 |
| 8. | Distribution curve of the particles collected on the four stages of the impactor | 35 |
| 9. | Distribution curve of the particles collected on the four stages of the impactor plotted on log-normal paper | 36 |
| 10. | Cumulative curve of the particles plotted on log-normal paper | 38 |
| 11. | Rosin-Ramler distribution | 40 |
| 12. | Distribution of the particles on each of the four stages of the impactor | 41 |
| 13. | Cumulative Curve of the particles from both Porton graticle and TGZ-3 Counting | 42 |
| 14. | Surface area Cumulative Curve of the particles | 44 |
| 15. | Volume Cumulative Curve of the particles | 45 |
| 16. | Electron Micrographs of the particles collected on stage 3 and 4 | 48 |
| 17. | Cumulative Curve for the particles measurements using both optical and electron microscope | 49 |
| 18. | Indulating land surface showing variety of strata (A,B,C and D) exposed | 54 |

| <u>Appendix</u> | <u>Title</u> | <u>Page</u> |
|-----------------|---|-------------|
| A | Mathematical Expression of the Log-normal distribution | 67 |

Chapter 1

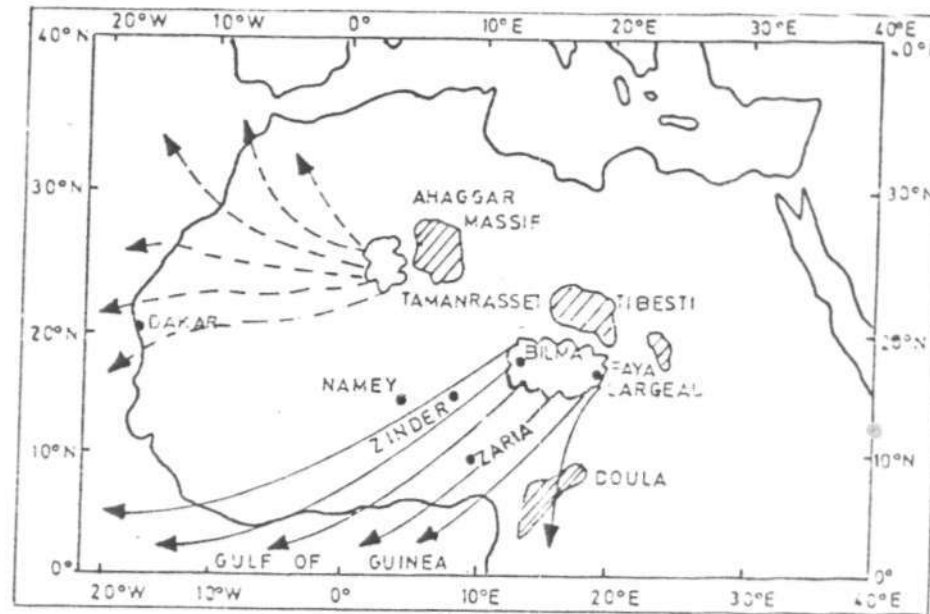
INTRODUCTION

The Harmattan season in the Northern part of Nigeria is always associated with dust laden atmosphere. The dust is commonly called Harmattan dust haze. The dust particles which are defined here as small discrete mass of solid earth matter are very fine and can remain suspended in the air for a long period of time. This phenomena has been observed annually between the months of November and March during which large quantities of dust particles are transported from the Sahara desert towards the Gulf of Guinea across Nigeria. The presence of these dust is indicated by a dusty atmosphere which reduces visibility to less than 1000 m as reported by Kalu (1979). The dust which affects the Nigerian zone, south of latitude 15°N , comes from North-Eastern sahara along the alluvian plain of Bilma (18°N , 12°E) in southern Niger and Faya - Largeau (18°N , 19°E) in Chad as depicted in Figure 1.

The harmattan dust particles are transported downward from the source region in the form of a 'plume' by the prevailing winds. It was reported by Aina (1972) that on the average it takes about twenty-four hours to reach the Northern part of Niceria.

1. 1. Generation of Harmattan Dust

The mode of production of Harmattan dust has not been extensively studied. However, there are so many different descriptions of the origin of the dust: It was reported by Yaalon and Ganor (1979) that the desert dust originates



LEGEND




-  Main source of dust
-  Trajectory in winter
-  Trajectory in summer

Figure 1: Trajectories of Harmattan dust Haze.
(From Kalu, 1979)

from wind erosion of alluvial deposits in the desert mountain valleys. Thus, the dust is produced as a result of chemical weathering of primary minerals. There is also the suggestion by Junge (1979) that some of the desert dust are produced by crystalline breakage of saltating grains, which depend on surface soil texture and wind speed. But generally, it has been accepted that the aridity of the sahara, the high temperature reached by its soil and the strong diurnal thermic turbulence resulting from the former are all factors which favour the production of the dust and its subsequent suspension in the atmosphere. Thus it is possible only when certain synoptic features occur over the source region (Adefalalu, 1968). One of such features is the development of high wind speed at the surface to create the necessary turbulence and instability required to keep the dust airborne for a considerable length of time.

The plume concept was generally accepted, as reported by Prospero (1972) and Kalu (1979), that it is not the atomistic conception that cause significant effect but rather the bulk plume form. The plume is made up of three phases, namely:

- i) The Instantaneous Phase: It is the period when dust particles are violently raised from the ground usually in the form of dust storms as a result of very strong surface winds.
- ii) The Spreading Phase: In this phase, transportation starts in the horizontal direction which marks the beginning of the spreading phase. This is followed

simultaneously by the deposition of heavier particles along the route by simple gravitational action. The wind gradually weakens and the plume loses its vertical momentum which makes it to spread.

- iii) The Equilibrium Phase: It sets in as soon as the spreading phase is concluded. At this point the plume has lost independence and moves entirely under the influence of the prevailing winds. This stage is usually marked by a gradual reduction in visibility within a few hours. After which visibility continue to deteriorates rapidly becoming poorest when the core of the plume comes over the station. This occurs at some hundreds of kilometers away from the source areas in the direction of the trade winds (Kalu, 1979). The rate of deposition increases greatly at this stage as a result of a vertical downward mixing caused by vertical pressure changes. Which is also a function of the distance from the source region, soil texture, wind speed and temperature.

1.2 Possible Effects of Harmattan Dust Haze

Several effects of the Harmattan haze includes environmental, climatic, health and so on.

- 1.2.1 Environmental Effects: Harmattan dust haze has numerous environmental effects, the most easily noticeable among them is the reduction in visibility, which marks the arrival of the dust haze. Reduction in visibility causes a lot of inconveniences in civil aviation as

sometimes it either causes closure of airports temporarily or flights re-scheduled to early morning hours when vertical mixing of the atmospheric column has been suppressed due to low insolation.

Other ecological effects include nutrient input to the soil via dust deposition which subsequently changes the physical soil structure and composition required for plant growth. Furthermore, the deposition of the dust into ocean waters and rivers may affect marine life. It was indicated by Lundholm (1979) that deposition of nutrients associated with Saharan dust into ocean waters contribute significantly to the productivity of the surface waters.

- 1.2.2 Climatic effects: There are two ways in which an aerosol can influence the radiation budget. One is a direct way, by scattering and absorption of radiation. These are significant only for aerosols in the size range from 0.1 to 2 μm (Friedlander, 1977). The indirect way is by modifying the optical properties, particularly the albedo of clouds (Junge, 1979), since aerosols of radius greater than 0.1 μm act as condensation nuclei during cloud formation.
- 1.2.3 Health effects: The deposition of Harmattan dust particles with its different mineral composition and shapes through the respiratory tract certainly affect human health and that of other animals. However Friedlander (1977) has indicated that the fraction

deposited depends on the lung geometry and air flow patterns of individuals as well as size ranges of the particles.

1.3 A review of Previous Work on Saharan Dust

A lot has been written about the transport and deposition of the saharan dust in various parts of Africa. Some of these studies include the transport and deposition over eastern sahara by Wilson (1972) and the movement of the saharan dust in summer by Carlson and Prospero (1972). Furthermore, the long range transport of the saharan dust has been studied by Schütz (1979).

However, the published materials about West Africa have concentrated on evolving forecasting techniques for the on set and dispersion of Harmattan dust. These include the study of the variation of visibility during harmattan periods by Adetunji et al; (1979). Bigglestone (1958) had studied the diurnal variations in the surface wind speed at Kano. While Samways (1975) has reported a synoptic occurrence of Harmattan haze at Kano. In addition to these, studies have been carried out on the mineral/elemental composition of the saharan dust by Prospero and Carlson (1970), Rahn et al; (1979) and by Adetunji and Ong (1980) with X-ray diffractometer. A microscopical analysis of the harmattan dust at the Imperial Institute, London as well as the mechanical sifting analysis were done by Hamilton and Archbold (1945).

Mass and number size distribution studies were done by

Schütz and Jacnicke (1974). Patterson and Gillette (1977) carried out size distributions measurement of soil-derived aerosols at Colorado, while the determination of size distribution of coarse-grained and fine grained were carried out by Gillette and Walker (1977).

As part of a broader study of the Harmattan haze, in this project the mineralogical composition as a function of size range was determined. The samples were collected on a four-stage cascade impactor. In addition the number-size distribution were studied by counting and sizing of micrographs of both optical and transmission electron microscopes for comparison. The counting and sizing was done with both Carl Zeiss Counter and Porton graticule for comparison. Log-normal distribution has been chosen in this work because this could reveal useful information about the various component sources involved in the formation of Harmattan dust. The log-normal type of distribution made it possible to evaluate certain representative constants of the particles which have been used to make accurate calculations of certain particulate properties such as the shape factors.

1.4 Particle Size Distribution

Dust particles encountered are usually irregular in shape and as such, the sizes assigned to them are defined arbitrarily. Their significance depends on the manner in which they are measured. Sizes related to particle geometry are usually statistical in nature in that reliable measurements require that either a repeated measurement is done on each particle at a number of different orientations or

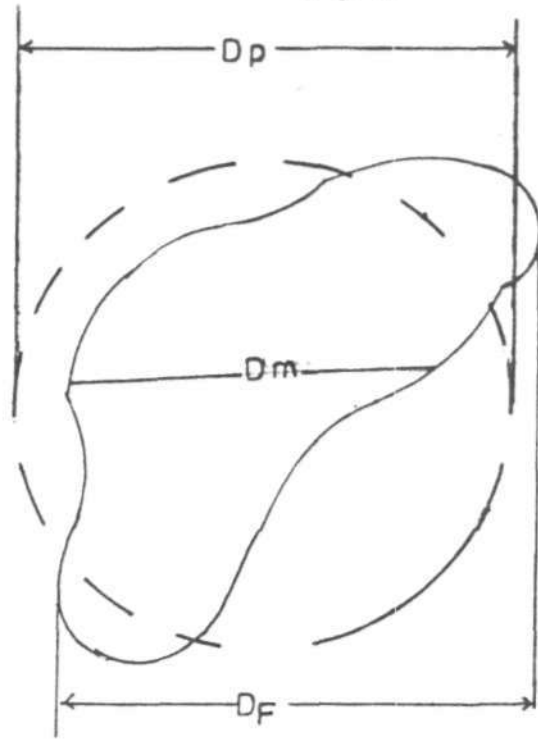
that a number of similar particles be measured at random orientations. The latter is employed in this work since it will be difficult to make measurements of dust particles at different orientations.

There are three well-known statistical geometric diameters which are usually assigned to a particle of irregular shape when viewed in an optical or electron microscope. These are based on the classification in the IAEA Technical Reports No.179 (1978). They are as follows:-

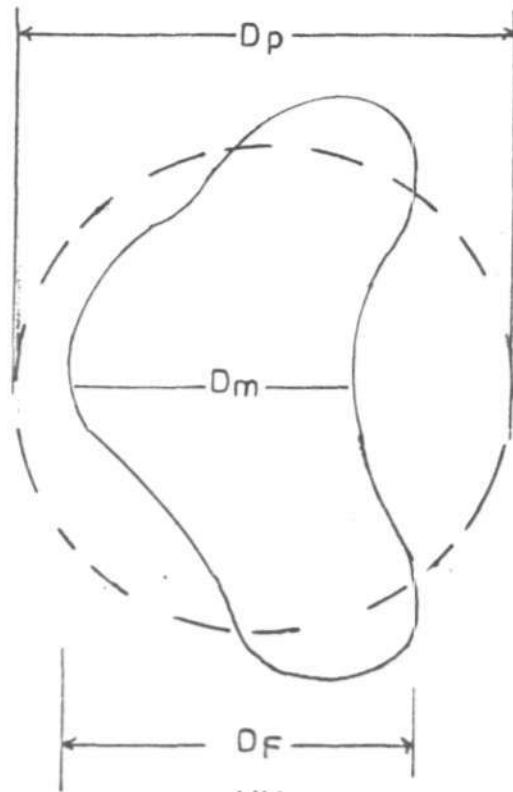
- i) Martins diameter (D_M): This is the length of a chord, parallel to a given reference line that divides the profile into two equal areas as shown in Figure 2 below.
- ii) Feret's diameter (D_F): It is the length of the projection of the profile onto a fixed reference line.
- iii) Projected area diameter (D_p): This is the diameter of a circle having an area equal to that of the profile.

However, in this work, projected area diameters are measured by sorting out photo or electron micrographs profiles of the particles into different size intervals. D_p is normally chosen because it is found to be independent of the orientation of the particle as depicted in Figure 2 (i and ii).

A detailed particle size distribution studies can help in predicting the behaviour of aerosols released to the environment, in designing filtration systems and in evaluating the hazard associated with inhalation of a



(i)



(ii)

Fig.2 Showing three different types of diameters assigned to particles in different orientations (i) and (ii)

particular aerosol or a certain concentration of it.

It has been generally accepted that there is no single distribution that fits in a data perfectly. However, it was suggested by Jacnicke and Davies (1976) that any choice of size distribution should satisfy at least one of the following criteria.

- (i) There is a physical reason(s) for the choice of the type of equation to describe a distribution.
- (ii) The mathematical expression selected should be as simple as possible, so as to reduce a bulky set of data to a few important numbers.
- (iii) The mathematical description should approach the measured values with minimum deviations.

Although there are various types of distributions employed in a particle size work, only the ones commonly encountered will be reviewed briefly.

Studies made by Junge (1955) from impactor samples and direct optical microscope counts showed that the size distribution function dN/dr is proportional to the inverse of the fourth power of the radius r^{-4} for particles of radii (r) greater than $0.5 \mu\text{m}$. Friedlander and Pasceri (1965) have found from measurements of aerosols of radius greater than $0.4 \mu\text{m}$ using four stage impactor, that the slope of the size distribution function dN/dr , for outdoor samples varied over the range 0.1 to $20 \mu\text{m}$. That for an indoor sample however, was closely proportional to r^{-4} . They suggested that such similarities in size distributions can

be explained by the existence of certain special solutions to equations which describe the rate of change of particle size distribution with time. The solutions were termed "self-preserving" theory, the size distribution function for radii greater than about $0.05\mu\text{m}$ is given by

$$\frac{dN}{dr} = 0.05 \phi r^{-4} \quad \text{-----} \quad 1.4.1$$

where ϕ is the particle volume per unit volume of aerosol.

The shape of the self-preserving distribution (SPD) was shown by Junge (1969) to differ from that of the observed distributions, especially in that the slope beyond the maximum is much steeper than r^{-3} . He also showed that the change with time of the SPD is very slow compared with meteorological time scales for all radii greater than $0.1 \mu\text{m}$. Furthermore, the SPD was found to be mathematically complex.

Friedlander (1960) introduced an explanation for the atmospheric aerosol size distribution which is different from that of SPD. Whereas SPD applies to a single process such as coagulation, the concept introduced by Friedlander referred to as "Quasi-stationary distribution" (QSD), for which the effects of two or more processes are balanced. It was indicated that QSD's approach to atmospheric aerosols can only be expected if

- (i) Gain and Loss processes of aerosols balance each other.
- (ii) The net rate of these processes is higher than the rate of change of meteorological conditions.

Later it was shown that because of the difficulty in fulfilling the above conditions QSD was also found to be

inadequate in describing the observed similarities of the aerosol distribution for radii greater than 0.1 μm .

The distribution was furthermore expressed by a formula by Junge (1963). It was based on the fact that aerosol of varied origin combine to form a coherent size distribution given by

$$\frac{dN}{d \ln r} = C r^{-\beta} \quad \text{--- 1.4.2}$$

where dN is the number of particles per cm^3 in the range $d \ln r$.

C is a constant depending on the total number N , of the particles per cm^3 . The value of β is about 3 for radii less than 10 μm and 6 for radii greater than 10 μm .

Subsequently, it was found that Junge distribution applies to particles of radii between 0.1 and 1 μm . Those of radii from 1 to 10 μm have only a slight effect on it, while those from 10 to 100 μm have no effect at all. Since the size of atmospheric aerosols covers about three powers of magnitude, which cannot be covered by this type of distribution, another distribution has to be obtained which will fit all the powers of magnitude of aerosol size.

The log-normal distribution has the advantage that it can cover the change of steepness usually observed between the size ranges 0.1 to 1 μm , 1 to 10 μm and 10 to 100 μm .

The distribution is given by

$$\frac{dN}{d \ln r} = \frac{N}{\ln \sigma_g \sqrt{2\pi}} \cdot \exp \left[-\frac{(\ln D - \ln D_0)^2}{2 \ln \sigma_g} \right] \quad \text{--- 1.4.3}$$

where N is the number of particles per unit volume having diameter between D and $D+dD$, $\ln\sigma_g$ is the standard deviation of $\ln r$. D_m is the median diameter of the particles. The log-normal distribution possesses unique mathematical properties which makes it easy to handle, for example, the distribution of all powers of the radius have the same value of geometric standard deviation, σ_g . Similarly, distributions of complex aerosols resulting from combination of multiple independent sources, can be analysed by method of curve fitting to reveal the individual contributions of the component sources as described by Davies (1974).

Log-normal distribution has been chosen in this work because of the above mentioned advantages. In cases where a log-normal distribution or one of its modification fail to fit the data, certain empirical equations can be used. For example the Rosin-Rammler equation.

$$P = 100 \exp (-D/C)^b \quad \text{1.4.4}$$

where C and b are constants and P is the percent of particles having a size larger than D .

As mentioned above the Rosin-Rammler equation is purely empirical and relies heavily on curve fitting. Thus only one distribution cannot be used to obtain the various statistical measures. Finally, there are other intricate size distribution equations that are only applicable in extremely special cases.

Chapter 2

CENTRAL THEORY AND SOURCE OF ERROR IN AEROSOL SAMPLING

2.1

2.1 Introduction

The purpose of any sampling programme is to obtain a representative sample of the particle population. A representative sample as defined by Peterson (1972) is that in which the properties of the aerosol such as concentration, size distribution, chemical composition and so on are not changed by sampling from the total gas system. In general, the following points are considered for sampling an aerosol system.

- (i) The purpose of the sampling activity and the information needed to fulfil the objective.
- (ii) The general character of the aerosol to be sampled with the emphasis on the possible size and concentration of the particles.
- (iii) The sampling equipment or collecting media to be used.
- (iv) The duration of sampling.

Sampling of aerosol can be done either in still air or dynamic air; however, the best form of sampling is done with as little disturbance to the character of flow of the total gas as possible. Thus the isokinetic method proposed by Zebel (1976) is recommended. The isokinetic sampling is achieved when the sampling air speed into the sampler is equal to that of the approaching air stream. Otherwise the sampling is an-isokinetic. If the sampling speed is too high, there will be a deficiency

of coarse particles. And if a too low sampling speed is used, an excess of coarse particles are collected. But it should be noted that isokinetic is difficult to achieve because both the flow rate and the direction of the wind are not always constant. So in cases where isokinetic is not achieved, correction has to be made for an-isokineticity.

The following formula for estimating the sampling error for non-isokinetic conditions was suggested by Davies (1968).

$$C_s/C_a = 1 + \left[(V_a/V_s) - 1 \right] \cdot f(st) \quad \text{--- 2.1.1}$$

where C is the concentration, V is air speed, the subscripts a and s refer respectively to air and sample, f(st) is a function of stokes number (st)

$$f(st) = 2 St / (1 + St) \quad \text{--- 2.1.2}$$

$$St = \frac{2F}{LW^2} mB \quad \text{--- 2.1.3}$$

For rectangular jets of length (L) and width (W) and F is the volumetric flow rate through the jet. $mB = \tau$ called the relaxation time, is given by the expression below

$$\tau = 3.0 \times 10^{-6} \rho_p D^2 K_s \text{ (secs)} \quad \text{--- 2.1.4}$$

where ρ_p is the density of the particle

D is the diameter of the particle

K_s is the Cunningham's correction factor.

The IAEA Technical Reports No.179 (1978) gave Cunningham's correction factor as

$$K_s = 1 + (2/pD) (6.32 + 2.01 \exp^{-0.1095 pD}) \quad \text{--- 2.1.5}$$

where P is the air pressure in cm of Hg

D is the diameter of particle in μm .

In this report, sampling was done an-isokinetically and the error due to this type of sampling for each stage of the sampler was calculated using equations 2.1.1 to 2.1.5 where a unit density was assumed. The results obtained are shown in Table 1.

Table 1: Calculated values of an-isokinetic effect for each stage.

| Stage Number | J e t O r i f i c e | | Effect of an-isokinesis (Calculated) |
|--------------|---------------------|------------|--------------------------------------|
| | Length (cm) | Width (cm) | |
| 1. | 1.9 | 0.66 | 0.848 |
| 2. | 1.4 | 0.14 | 0.991 |
| 3. | 1.4 | 0.075 | 0.998 |
| 4. | 1.4 | 0.027 | 0.997 |

2.2 Instrumentation

Sampling instruments usually consists of a probe sucking in the air with the aerosol and a collecting part where the aerosol particles are deposited on filters or other devices. There are different types of sampling instruments in use today each based on one of the following phenomena: Inertial Impaction, Sedimentation and Brownian movement (diffusion) of particles.

2.3 Sampling

The sampler employed in this work is a four stage Casella MK 2a Cascade impactor, oriented to face the North-Eastern direction. The site was on top of 10 metre-high

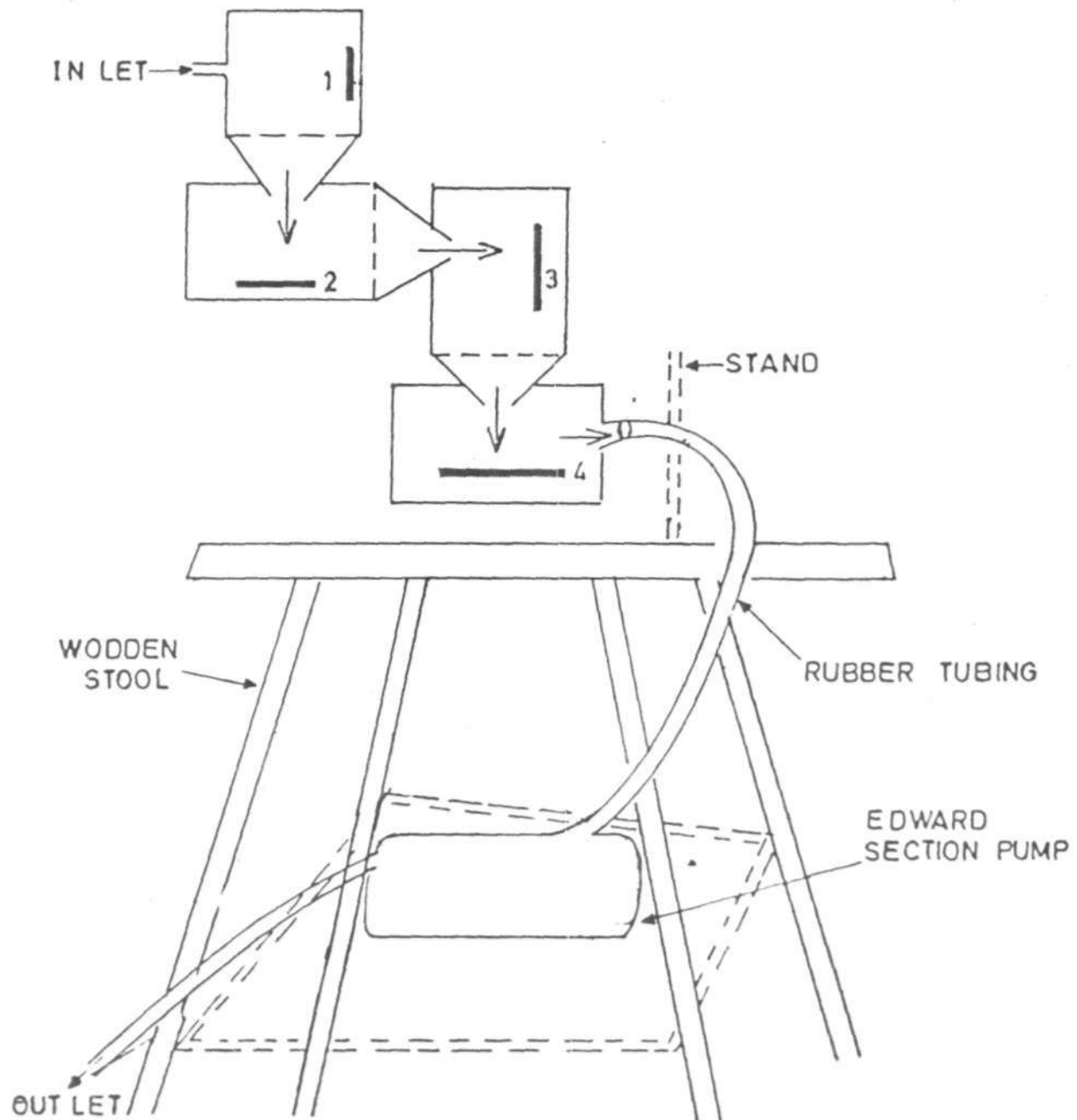


Fig. 3 : Arrangement of the sample collector placed on top of Dept. of physics laboratories building

physics building of Ahmadu Bello University, Zaria. The sampler was raised to such a high level so as to make sure that only dust of Harmattan origin was collected. Also the sampler was firmly clamped to a wooden stool as shown in Figure 4, to avoid its displacement as a result of high winds. The impactor was then connected to an Edwards suction pump with a rubber tube. The pump was operated at aspiration rate of 10 litres per minute.

Harmattan dust samples were collected on 25 mm diameter glass discs previously coated with Formvar film. The glass discs are covered with a petri-dish before and after collection of the sample to reduce the chances of contamination from other sources. Collection time varies from twenty-four hours to seventy-two hours depending on the concentration of Harmattan dust for a period lasting from January to February as shown in Table 2. The data of wind speed and visibility for the days of collection were obtained from Institute of Agricultural Research (IAR) Weather Office, Zaria.

The sample collected in this way were analysed to determine the mineral composition of the dust and the number size distribution of the particles.

Table 2: Mass of the samples collected and the Period of Collection

| From | To | Mass ($\times 10^{-3}g$) Collected | Time (Hours) | Wind Speed (m/s) | Visibility (km) |
|---------|---------|---|-----------------|------------------------|--------------------|
| 15-1-86 | 16-1-86 | 1 - 13 | | | |
| | | 2 - 16 | 36 | 2.71 | 1 |
| | | 3 - 21 | | | |
| | | 4 - 14 | | | |
| 16-1-86 | 17-1-86 | 1 - 07 | | | |
| | | 1 - 11 | 24 | 2.03 | 10 |
| | | 3 - 14 | | | |
| | | 4 - 10 | | | |
| 17-1-86 | 20-1-86 | 1 - 11 | | | |
| | | 2 - 16 | 20 | 1.85 | 1 |
| | | 3 - 19 | | | |
| | | 4 - 12 | | | |
| 20-1-86 | 23-1-86 | 1 - 13 | | | |
| | | 2 - 15 | 34 | 1.39 | 2 |
| | | 3 - 10 | | | |
| | | 4 - 11 | | | |
| 23-1-86 | 27-1-86 | 1 - 7 | | | |
| | | 2 - 10 | 72 | 1.31 | 18 |
| | | 3 - 10 | | | |
| | | 4 - 11 | | | |
| 31-1-86 | 03-2-86 | 1 - 03 | | | |
| | | 2 - 03 | | | |
| | | 3 - 05 | 60 | 1.40 | 40 |
| | | 4 - 06 | | | |

| | | | | | |
|--------|--------|-------|----|------|----|
| 3-2-86 | 7-2-86 | 1 - 1 | | | |
| | | 2 - 1 | | | |
| | | 3 - 1 | 72 | 1.19 | 44 |
| | | 4 - 1 | | | |

| | | | | | |
|--------|---------|-------|----|------|----|
| 7-2-86 | 14-2-86 | 1 - 1 | | | |
| | | 2 - 1 | | | |
| | | 3 - 1 | 72 | 1.53 | 44 |
| | | 4 - 1 | | | |

QUALITATIVE X-RAY ANALYSIS

A given substance always produces a characteristic X-ray diffraction pattern whether that substance is present in pure state or as a constituent of a mixture of substances. Unlike other methods of chemical analysis, the X-ray diffraction analysis discloses the presence of a substance as it exists in the sample and not in terms of its elemental composition.

3.1 Sample Preparation

The method of sampling employed in this work gave rise to dust samples being collected settling in random orientation configuration. This is important in X-ray diffraction since non-random orientations of the particles introduces error in the diffraction patterns obtained (Vassamillet and King, 1967). The samples on the glass discs were then pressed slightly with a clean glass to remove surface roughness which can also introduce errors in the results.

3.2 Procedure of Identification of Minerals

The X-ray diffraction traces were obtained on a Philips PW 1140 diffractometer using $\text{CuK}\alpha$ radiation at a scan speed of $2^\circ 2\theta \text{ min}^{-1}$. The results from each stage obtained are shown in Figure 4.

Identification of the unknown minerals in the sample was done considering the fact that the pattern obtained for a substance constitutes a sort of fingerprint by which

substance may be uniquely identified. After obtaining the diffraction pattern of the unknown sample, the plane spacing, d , corresponding to each peak on the chart was obtained from Tables in the X-ray diffraction search manual which give d as a function of 2θ for various characteristic wavelengths.

A scale of expected minerals was constructed which gives relative intensities as a function of line position when laid on the diffractometer chart. The scales were prepared from values obtained from index cards for expected minerals given in the data file of Joint Committee on Powder diffraction standards (JCPDS). These scales were compared with the XRD trace obtained from the sample. Where the trace and the scale match indicate that a particular mineral is present in the sample. The procedure was repeated for all expected minerals until the composition of the sample was determined. The analyses of the XRD trace from each stage was found to consist of the following as shown in Table 3.

Fig. 4: X-ray diffraction traces of the sample collected on the four stages of cascade impactor

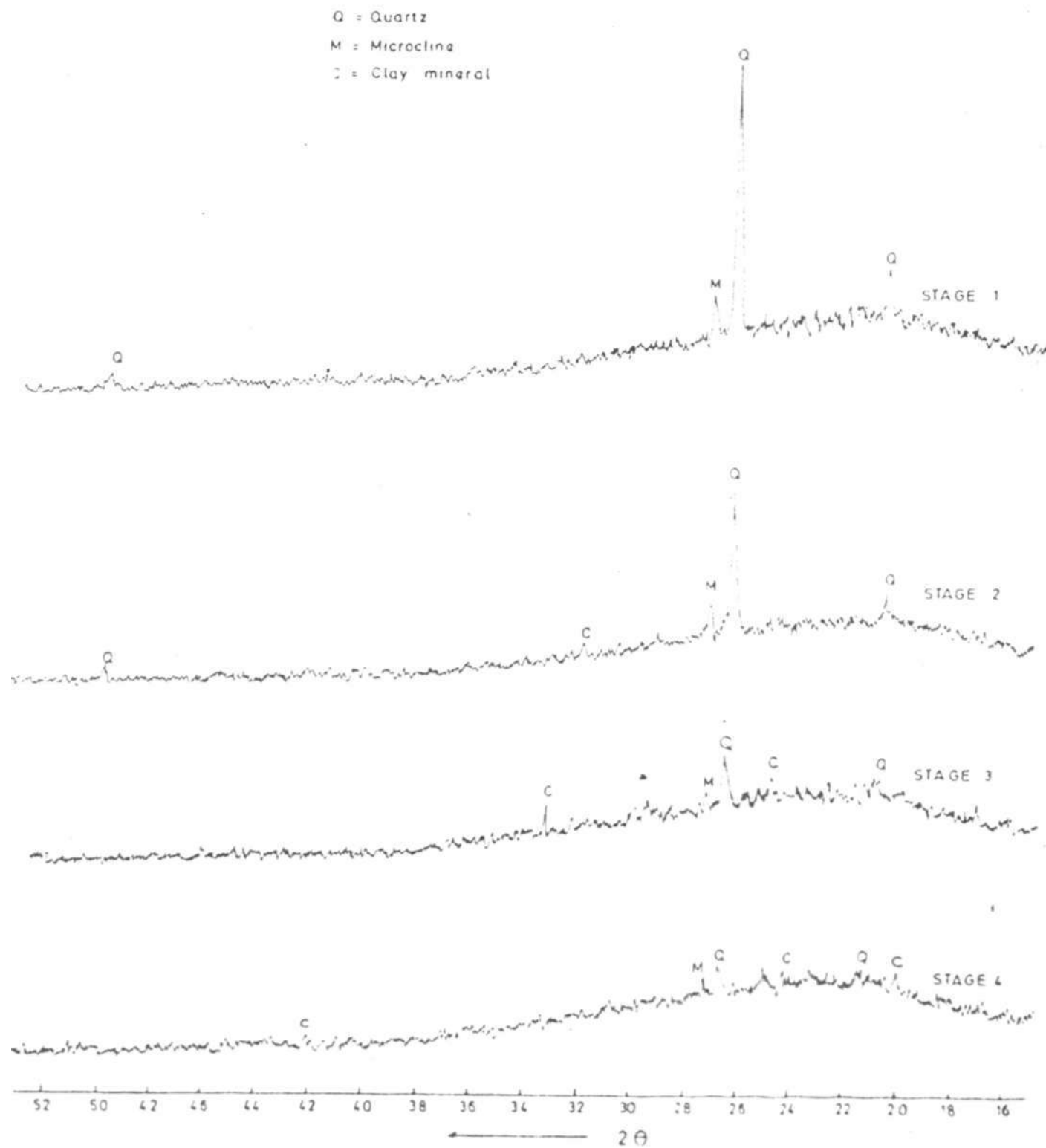


Table 3 : Showing mineral composition of Harmattan dust on each stage.

| CASCADE IMPACTOR STAGES | | | |
|--|--|--|--|
| 1 | 2 | 3 | 4 |
| (a) Quartz (SiO ₂) | Quartz (SiO ₂) | Quartz (SiO ₂) | Quartz (SiO ₂) |
| (b) Microline (KA ₁ Si ₃ O ₈) | Microline (KA ₁ Si ₃ O ₈) | Microline (KA ₁ Si ₃ O ₈) | Microline (KA ₁ Si ₃ O ₈) |
| (c) - | - | Small proportion of Clay minerals (Kaolinite, Illite etc) | Equal proportion of Clay Minerals with the other above minerals. |
| (d) - | Peak height reduced by about 50% | Peak height reduced by about 75% | Peak height reduced by about 90% |

This result is interesting and will be discussed in Section 6.1.

Chapter 4

EXPERIMENTAL TECHNIQUES FOR SIZE DISTRIBUTION MEASUREMENTS

There are various methods employed in the measurements of size distribution. The choice of particular method depends on the type of aerosol, method of sampling and the form in which the data will be presented. The samples collected with a cascade impactor are usually used for microscopic analysis. Two types of microscopes were used in this report, namely light and electron microscopes, for comparison of the results.

4.1 Analysis With the Light Microscope

In the optical work carried out, simple optical microscopy imaging were used to determine the number size distribution of the dust particles. The technique is feasible because of the resolving power of the instrument, which is of the order of $0.2 \mu\text{m}$ (Grundy and Jones, 1976).

The optical microscopy method does not require any special sample preparation, thus a convenient method. Photo micrographs were taken as a permanent picture of the sample. Counting and sizing were done using both Carl Ziess TCZ-3 Counter and Porton graticle for comparison.

4.1.1 Counting and sizing of dust particles

As mentioned in section 4.1 counting and sizing was done using electronic counter and Porton graticle so as to compare the results and find whether there is any marked difference between the two methods.

TGZ-3 Counting: This instrument enabled the author to count

and size the particle diameter by adjusting the size of the light spot to be equal to the projected area diameter of the particle. It is then recorded in the appropriate size interval provided by one of the windows of the counter. The instrument also record the number frequency of the particle in each size interval. The 48 size intervals on the windows of the counter were then divided by the magnification of the particles to obtain the actual size intervals of the particles.

Porton graticule counting: In this method of sizing, a direct visual comparison of the diameters on the micrographs was done with the circles of the graticule. The graticule is a circular glass disc with a series of circles arranged in a $\sqrt{2}$ progression (May, 1965) and series of squares at the centre. The measured diameters were recorded in the appropriate size intervals after conversion to the actual sizes of the particles. This was continued until the entire micrograph was covered. Noting the frequency of occurrence of each size interval. The results obtained gave the number frequency distribution of the dust particles.

4.1.2 Determination of shape factors

The values of the mean diameter were calculated from the size distribution obtained in Section 4.1.1. These values can then be used to determine other particulate properties such as surface area and volume of the particles which are required for proper characterisation of the dust particles.

These properties as defined by Robins (1954) are as

follows

$$\text{Surface area, } S, = \alpha_2 \overline{D^2} \quad \text{---} \quad 4.1.1$$

$$\text{Volume, } V, = \alpha_3 \overline{D^3} \quad \text{---} \quad 4.1.2$$

where α_2 and α_3 are called the surface area and volume shape factors. It was shown by Orr and Dallavalle (1959) that the values of α_2 and α_3 for spherical particles are π and $\pi/6$ respectively. For other irregularly shaped particles various values have been obtained which depend not only on shape but on orientation of the particles as well.

The expression for the ratio of the particle's projected diameter (D_p) and the the Stoke's diameter (D_s) was given by Robins (1954) in terms of surface area and volume shape factors as

$$\frac{D_p}{D_s} = \sqrt{\left[\frac{(\pi \times \alpha_2)^{\frac{1}{2}}}{6 \times \alpha_3} \right]} \quad \text{---} \quad 4.1.3$$

The value of the ratio for various size range has significance in particle size analysis, especially in determining the mass and number distributions by Stoke's diameter.

The shape factors for each stage of the impactor were determined from the distributions measured using electronic counter and Porton graticule for comparison. The values obtained are discussed in Chapter 5.

4.2 Analysis with the Transmission Electron Microscope

The Electron microscope is one of the most versatile instruments used in the assessment of airborne particles. When more discernible information about small particles is required, the electron microscope is often recommended.

The advantage of the electron microscope is that of high resolution which was reported by Grundy and Jones (1976) to be up to about 10^4 times greater than that of light microscope. Also a better contrast is obtained with the electron microscope operated at higher magnifications than optical microscope. Thus, sizing of small particles at such magnifications will be more accurate with the electron microscope. However, most workers prefer to work with light microscopes because of the complex manipulations involved and the tedious specimen preparations required in the electron microscopy.

Transmission electron microscope (TEM) was used here to determine the size distribution of the particles. As the name suggest, this instrument requires the specimen to be thin enough to allow the transmission of electrons. The equipment can be operated in two modes, the transmission mode and diffraction mode. In this project, the transmission electron microscopy was fairly succesful but a lot of problems were encountered in the diffraction mode. This was due to non availability of flaky particles in the sample. Thus the original plans to investigate the possibility of amorphousation of the surface of the harmattan particles had to be discarded. In the transmission

mode, measurement of size distribution were done with Carl Zeiss TGZ-3 counter. The results obtained were compared with that of light microscopy.

4.2.1 Specimen preparation

The quality of any electron microscope image on the screen depends to a large extent on how the specimens are prepared. For best contrast and resolution all spurious atoms had to be removed, since matter is not entirely transparent to electrons.

Perforated copper grids of about 3 mm diameter with a square mesh of 200 per inch were used as support grids. The specimen collected on conducting Formvar film for support are then mounted on support grids.

Preparation of Formvar films: Formvar films were prepared on glass discs prior to the collection of the dust samples on each stage of the Impactor, using the following procedure.

- (a) The glass disc was cleaned with detergent solution and polished with a clean piece of silk. The degree of cleanliness to be found after several trials.
- (b) The glass disc was dipped in a 1% ^W/V solution of Formvar in chloroform and drained vertically on the filter paper.
- (c) The coated glass disc were then used to collect samples on each stage of the sampler.

After X-ray and light microscope analysis, the samples with the Formvar were stripped off for electron microscope analysis. The stripping was done by lowering the glass

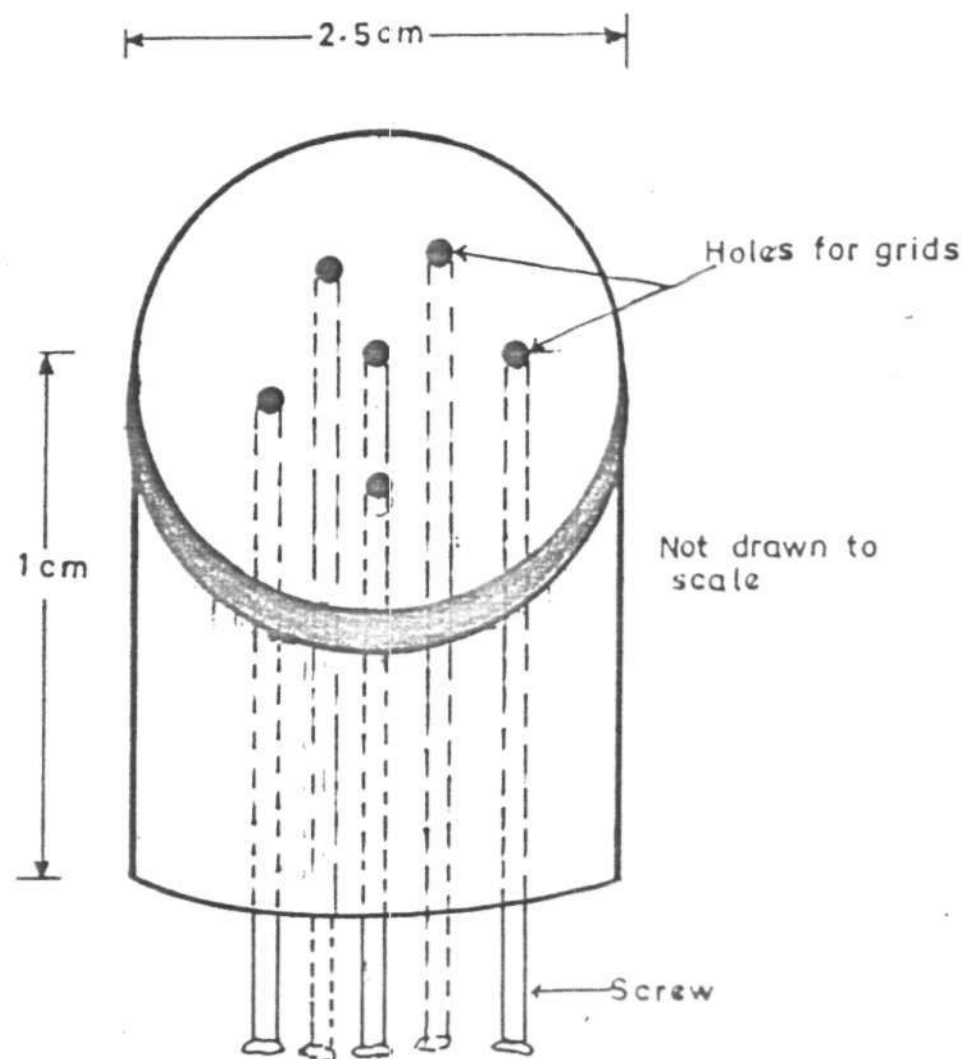


Fig. 5 : A metal jig for collecting film on the grids placed on the six holes

disc at shallow angle into a dish of distilled water. The film comes off the glass surface due to surface tension, and was floated on water. The films were found to part with the glass only after teasing up the edges as reported by Bradley (1967).

(d) The film was then collected on a Jig constructed at the Department of Physics Mechanical Workshop and shown in Figure 5) capable of holding six grids at a time. Each grid together with the film and sample was then retrieved using a sharp knife. The grids were later dried on a blotting paper.

Coating with evaporated Carbon: To remove surface change effects, the specimen was coated with evaporated carbon. The thickness of the coating did not exceed the 200 Å limit recommended to avoid serious loss of contrast.

A Polaron coating unity type E6432 was used to coat the specimen before it was inserted into the microscope. The equipment was operated at the electrode voltage of 8 Volts and was evacuated to a pressure of better than 10^{-4} mm of Hg, following the procedure in the operating instructions. A constant thickness of coating was maintained for all the specimen using the formula given below and illustrated in Figure 6.

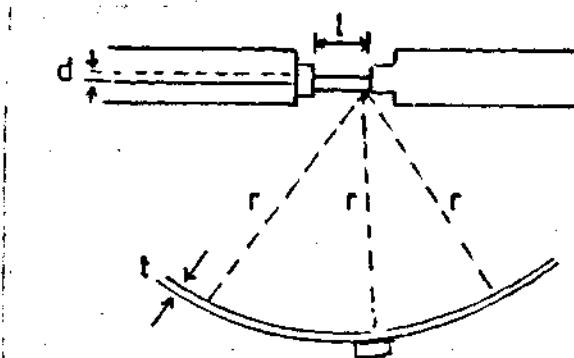


Figure 6: Arrangement used for evaluating thickness of coating

- l = length of carbon rod evaporated
- d = diameter of carbon rod
- r = distance of carbon tip from the grid
- p = density of carbon
- t = thickness of coating

$$\frac{d^2 lp}{4} = 4 r^2 tp \quad \text{--- 4.2.1}$$

$$t = \frac{d^2 l}{16r^2} \quad \text{--- 4.2.2}$$

where l = 2 mm
d = 0.5 mm
r = 4 cm

giving

$$t = 195 \text{ \AA} \quad \text{--- 4.2.3}$$

The coated specimen was then placed in the sample holder which was inserted into the microscope. A Philips EM 400T transmission electron microscope at accelerating voltage of 8 volts was used to obtain an image on the screen from which micrographs were taken.

The results of particle size measurements for comparison between optical and electron microscope counting are reported in Section 5.1.

Chapter 5

RESULTS OF PARTICLE SIZE MEASUREMENTS

Size distribution measurements of Harmattan dust was done using optical and transmission electron microscope methods. In both methods, micrographs were obtained and sized using an electronic counter.

5.1 Optical Microscopy Results

The sample for optical microscopy was collected as described in Section 2.2. Photomicrographs of the sample collected on the four stages are shown in Figure 7(a,b,c and d). It can be seen from the Figure that there is variation of size ranges from stage 1 to 4 with that of stage 4 being the smallest size range. Also there is non-uniformity of the sizes in any particular stage since each stage collects particles that falls within a particular size range.

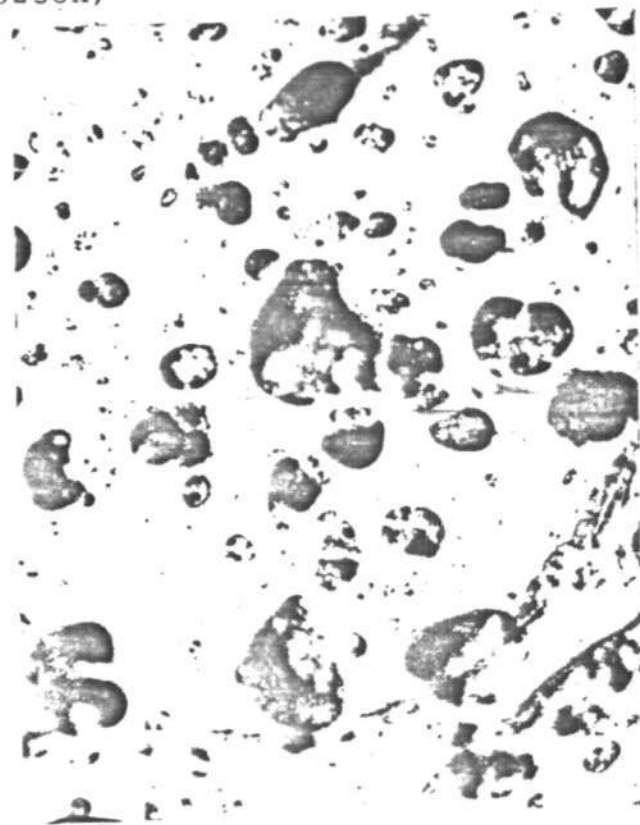
A plot of the number-size distribution of the particles from the four stages combined show an asymmetric frequency distribution which is skewed towards the lower values of the particle diameters as shown in Figure 8. However, when plotted on log-probability paper a symmetric distribution was obtained as depicted in Figure 9 which implies that the particles are log-normally distributed, having the following distribution function.

$$\frac{dN}{d \ln D} = \frac{N}{\sigma \sqrt{2\pi}} \exp \left[-\frac{(X - \mu_0)^2}{2\sigma^2} \right] \quad \text{--- 5.1.1}$$

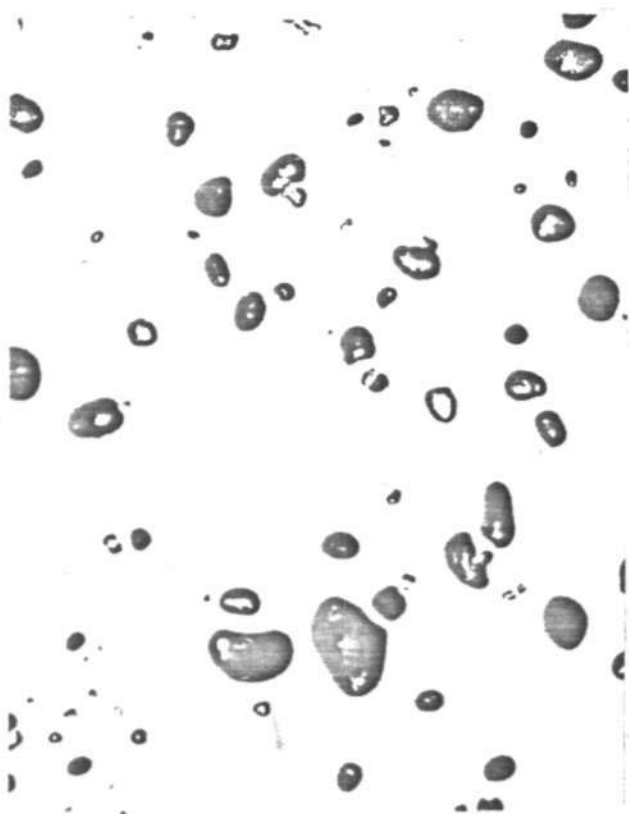
Figure 7: Photomicrographs of the particles collected on each of the four stages. Stage 1(a), Stage 2(b), Stage 3(c), Stage 4(d). (5238X)



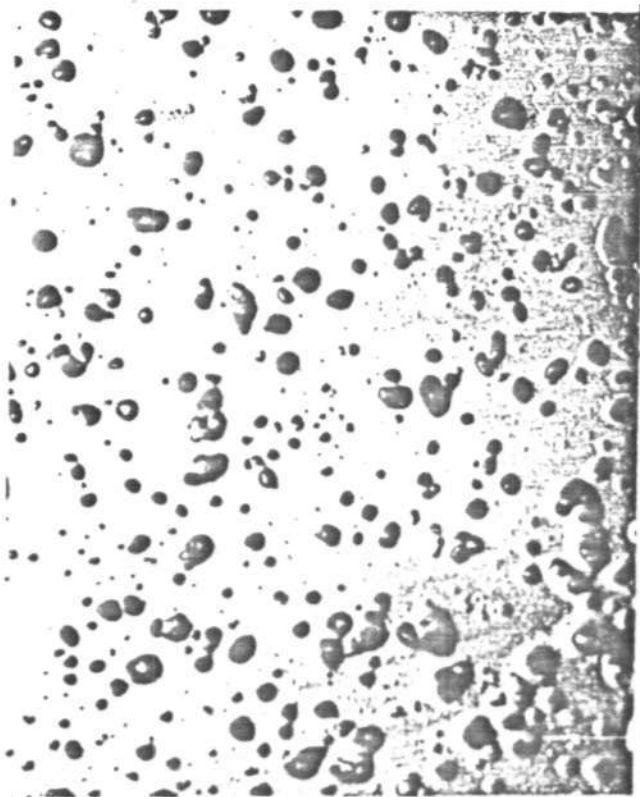
a



b



c



d

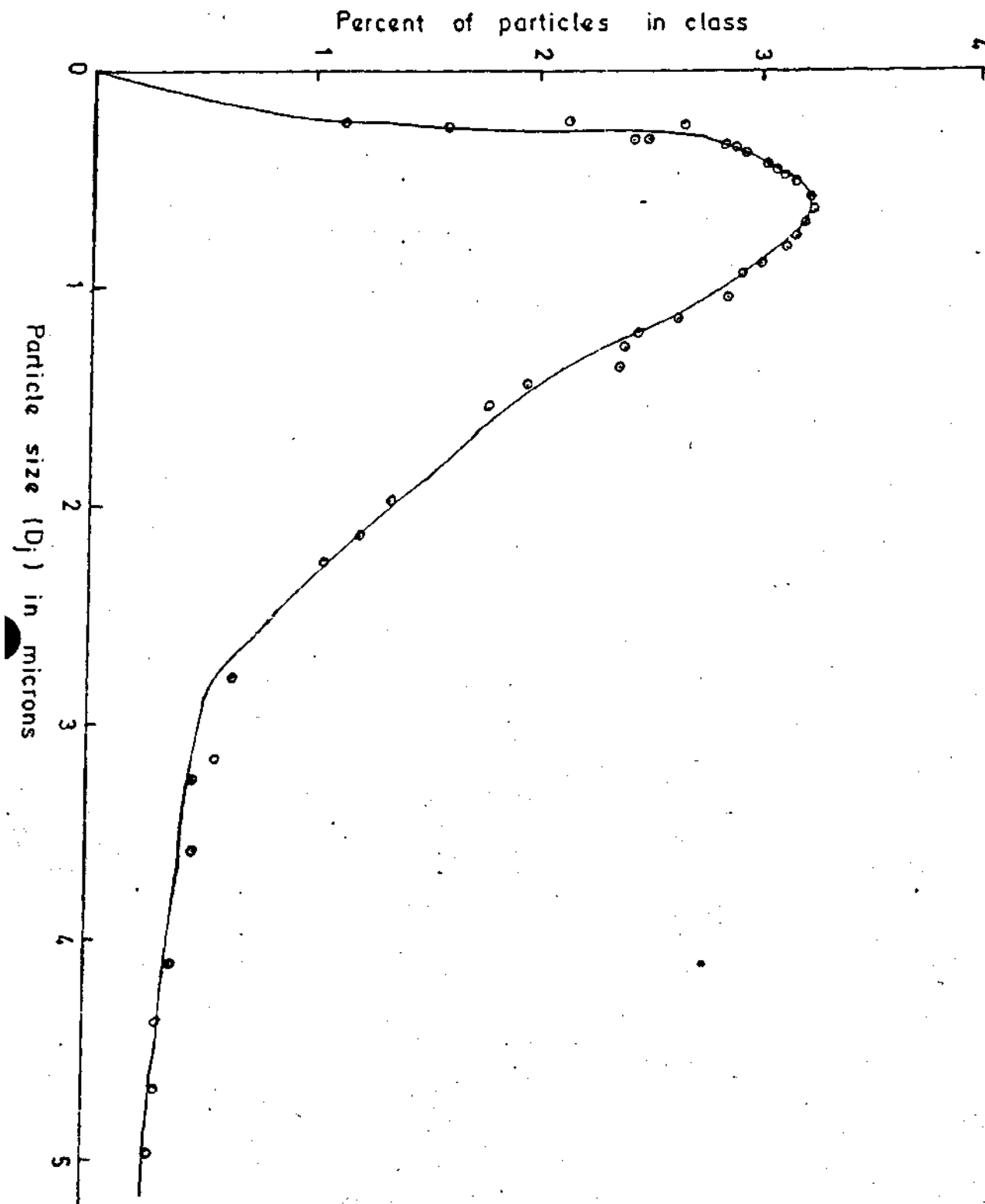


Figure 8: Distribution curve of the particles collected on the four stages of the impactor.

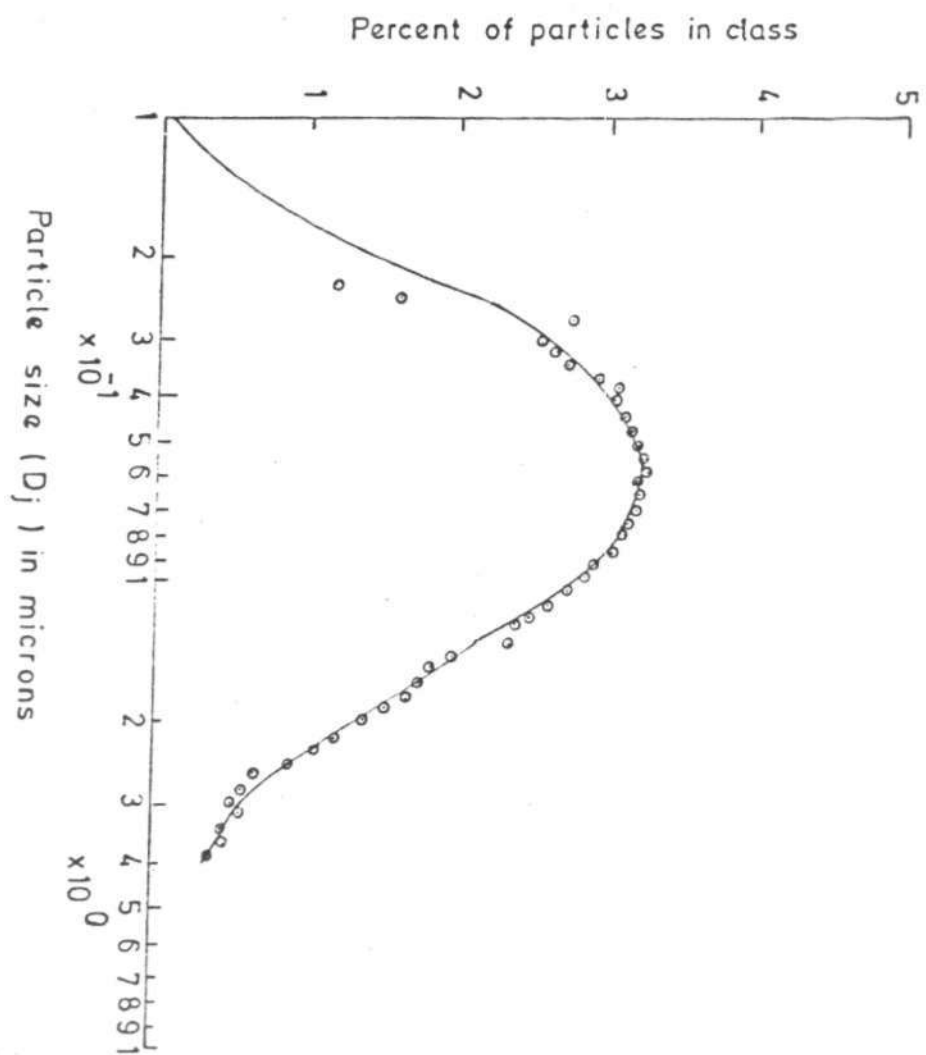


Figure 9: Distribution curve of the particles collected on the four stages of the impactor plotted on log-normal paper.

where $X = \ln D$
 $\sigma = \ln \sigma_g$
 $\mu_o = \ln D_{o,g}$

and σ_g is the geometric standard deviation and $D_{o,g}$ is the median or geometric mean diameter of the distribution and X and σ are the mean and standard deviation of the distribution respectively.

Furthermore, when the percent cumulative of the particle diameters was plotted against the upper value of the diameter intervals (D_j) on log-probability paper, a straight line was obtained as shown in Figure 10. The number of measurements n_i that falls in the i^{th} size interval for k intervals is related to the percent cumulative (P_j) by the equation;

$$P_j = \frac{100 \sum_{i=1}^k n_i}{\sum_{i=1}^k n_i} \quad \text{--- 5.1.2}$$

$D_{o,g}$ is the diameter at which the line intersects the coordinate $P_j = 50\%$.

Also

$$\sigma_g = \frac{\text{value of } D \text{ at } P_j = D_{84\%}}{\text{Value of } D \text{ at } P_j = D_{50\%}} \quad \text{--- 5.1.3}$$

$$\sigma_g = \frac{D_{84\%}}{D_{50\%}} = \frac{D_{50\%}}{D_{16\%}} \quad \text{--- 5.1.4}$$

Using values deduced from Figure 10

$$\sigma_g = \frac{1.68}{0.72} = 2.33$$

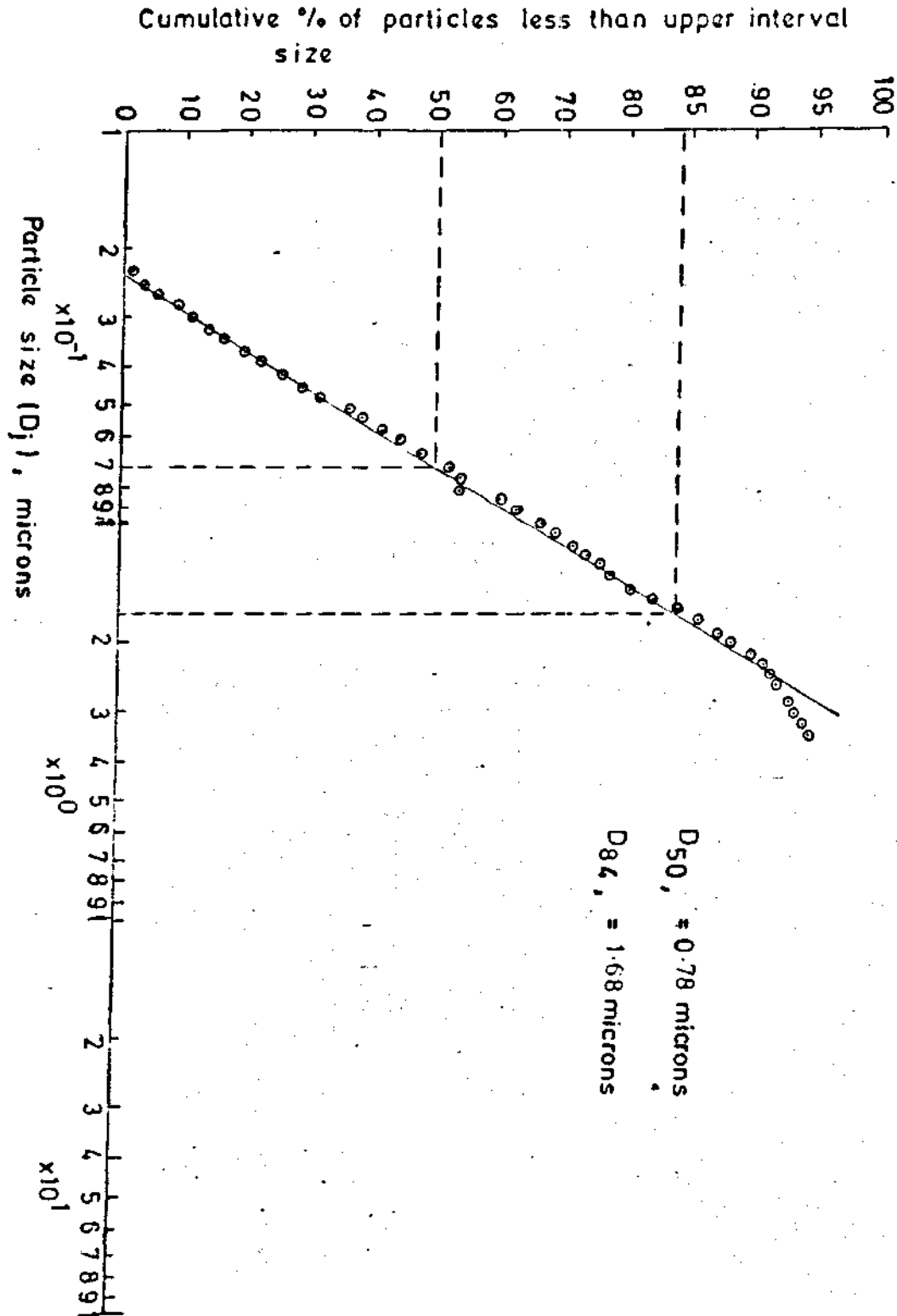


Figure 10: Cumulative curve of the particles plotted on log-normal paper

The mean diameter (\bar{D}) as derived in Appendix A is given by

$$\bar{D} = D_{o,g} \exp \left[\frac{\ln^2 \sigma_g}{2} \right] \quad \text{5.1.5}$$

and the mode (D_m) is given by

$$D_m = D_{o,g} \exp \left[\frac{- \ln^2 \sigma_g}{2} \right] \quad \text{5.1.6}$$

$$D_m = 0.35 \mu\text{m}$$

The deviation from straight line of the particles having larger diameter values, could be attributed to the method of sampling which sometimes leads to an abnormal log-normal distribution. However, Rosin-Rammler equation has been found to fit the data in this region. This yields a straight line when plotted on log-log paper as shown in Figure 11.

The distribution curve of the dust on each of the four stages was found to be skewed towards the lower values as shown in Figure 12. While the percent cumulative of the particles of each stage give a straight line when plotted on log-probability paper. The plots of percent cumulative for the particles sized using both TCZ-3 counter and Porton graticule are shown in Figure 13. The mean diameter values calculated using equations 5.1.4 and 5.1.5 for each stage are in Table 4.

Table 4: Mean diameter (\bar{D}) in microns for each of the 4 stages

| S I Z E R | S T A G E | | | |
|------------------------|-----------|------|------|------|
| | 1 | 2 | 3 | 4 |
| Semi-automatic Counter | 3.87 | 1.65 | 0.76 | 0.16 |
| Porton Graticule | 4.54 | 0.18 | 0.07 | 0.02 |

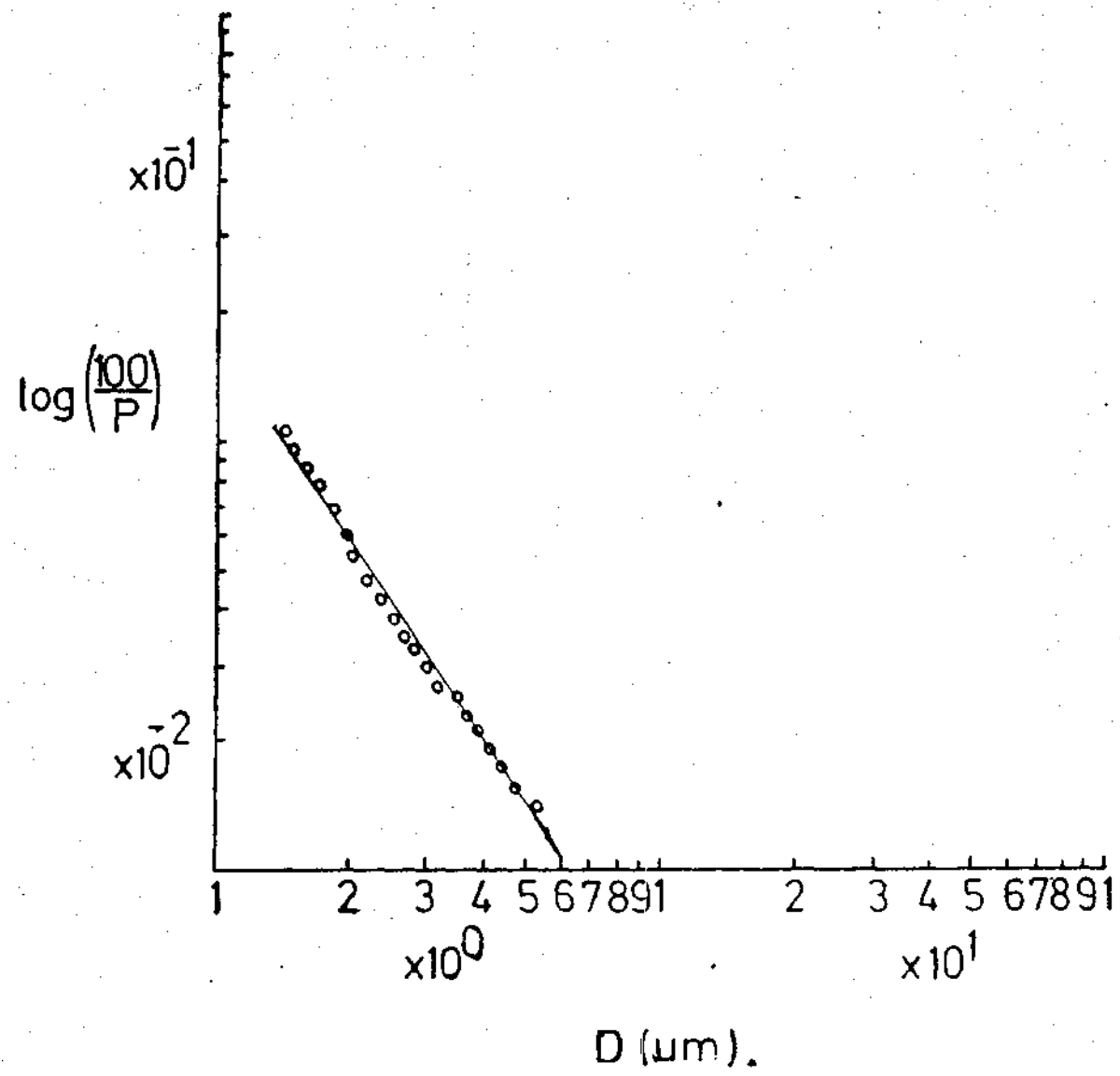


Figure 11: Rosin-Ramler distribution.

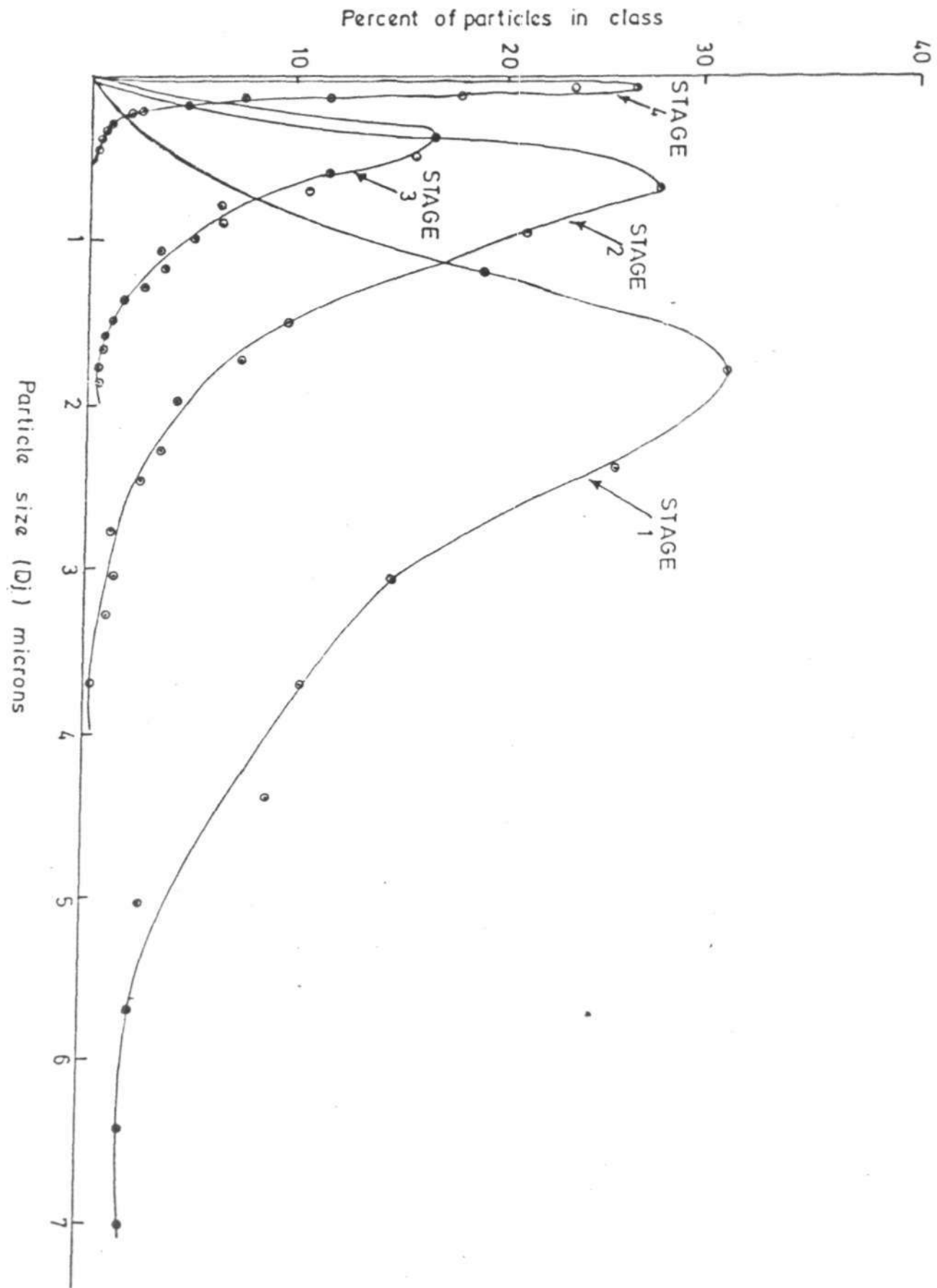


Figure 12: Distribution of the particles on each of the four stages of the impactor.

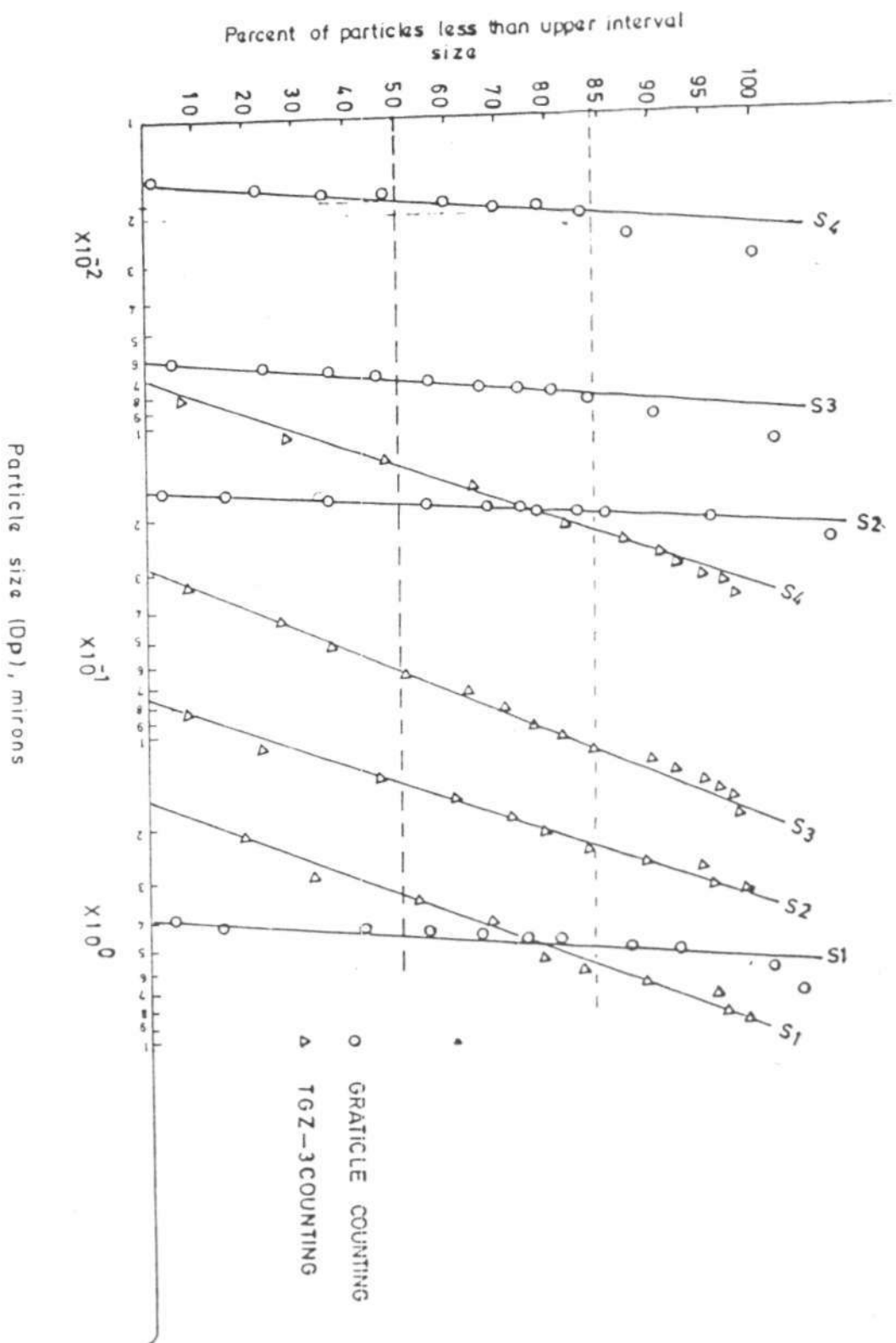


Fig.13 : Cumulative frequency curve of the particles from both portion graticle and TGZ — 3 counting

5.1.1 Calculation of shape factors

The diameter distributions for the particles on each stage obtained in Section 5.1 were converted to surface area and volume distributions by multiplying the diameters with πD and $\pi D^2/6$ respectively.

Plots of percent cummulative against surface area and volume of the particles were made to obtain the mean surface area (\bar{S}) and mean volume (\bar{V}) of the distribution as shown in Figures 14 and 15. These plots gave straight lines as expected from the properties of log-normal distributions.

Also

$$\bar{S} = S_{0,g} \exp \left[\frac{\ln^2 \sigma_s}{2} \right] \quad \text{--- 5.1.6}$$

$$\bar{V} = V_{0,g} \exp \left[\frac{\ln^2 \sigma_v}{2} \right] \quad \text{--- 5.1.7}$$

Where $S_{0,g}$ and $V_{0,g}$ are the surface area and volume at 50% cummulative and σ_s and σ_v are the geometric standard deviations of the surface area and volume distributions respectively. Similarly,

$$\sigma_s = \frac{S_{84\%}}{S_{50\%}} \quad \text{--- 5.1.8}$$

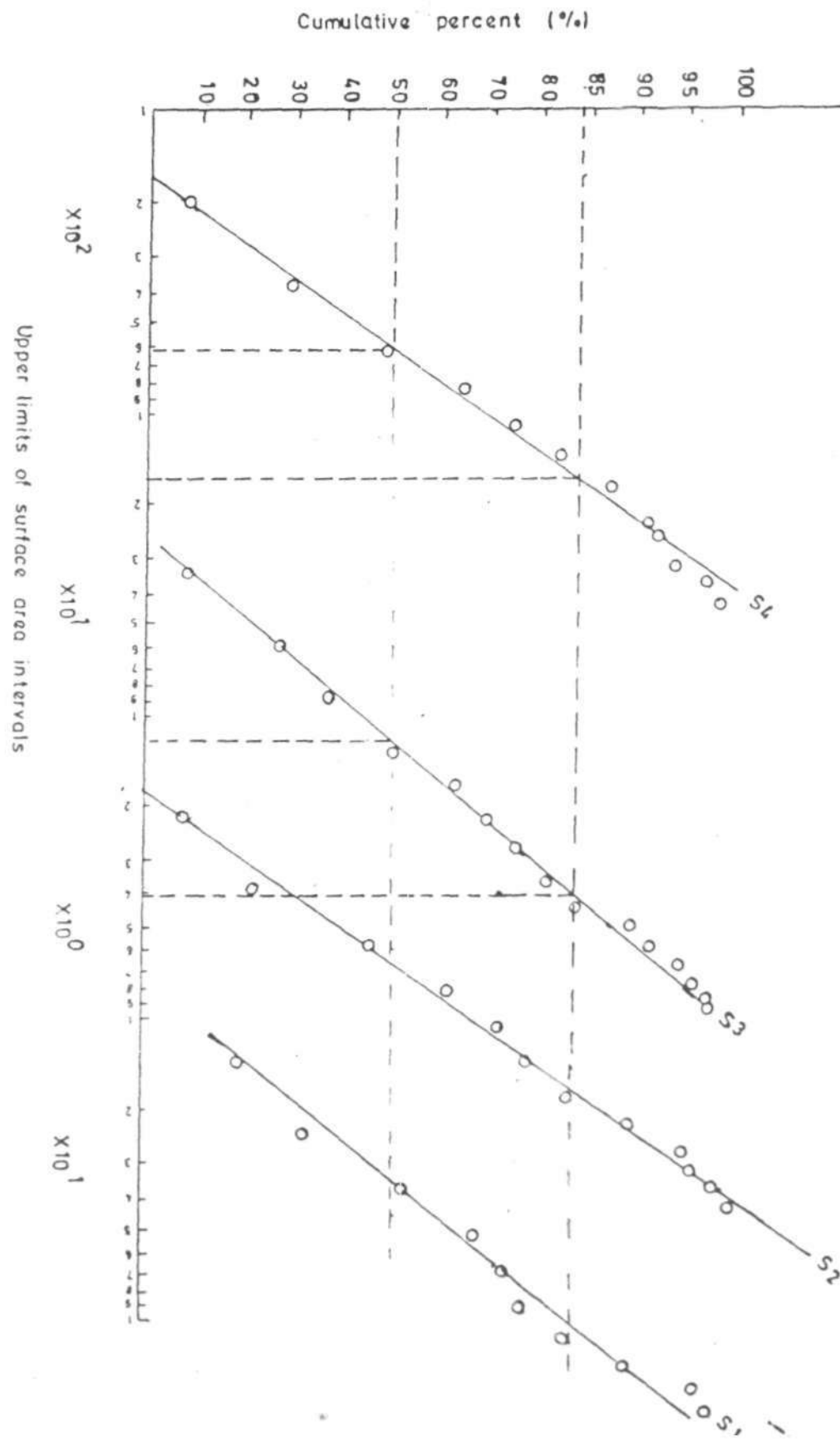
$$\sigma_v = \frac{V_{84\%}}{V_{50\%}} \quad \text{--- 5.1.9}$$

Also from Appendix A

$$\bar{D}^2 = D_{0,g}^2 \exp \left[\frac{4 \ln^2 \sigma_g}{2} \right] \quad \text{--- 5.1.10}$$

$$\bar{D}^3 = D_{0,g}^3 \exp \left[\frac{9 \ln^2 \sigma_g}{2} \right] \quad \text{--- 5.1.11}$$

Figure 14: Surface area Cumulative Curve of the particles.



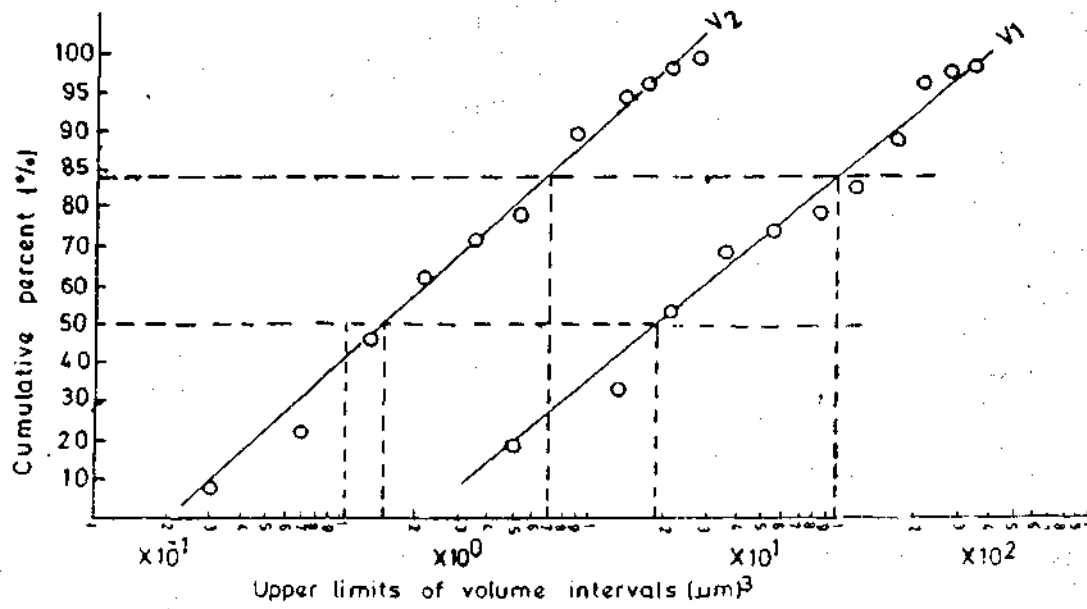


Fig.15a Volume cumulative curves for stage 1 and 2

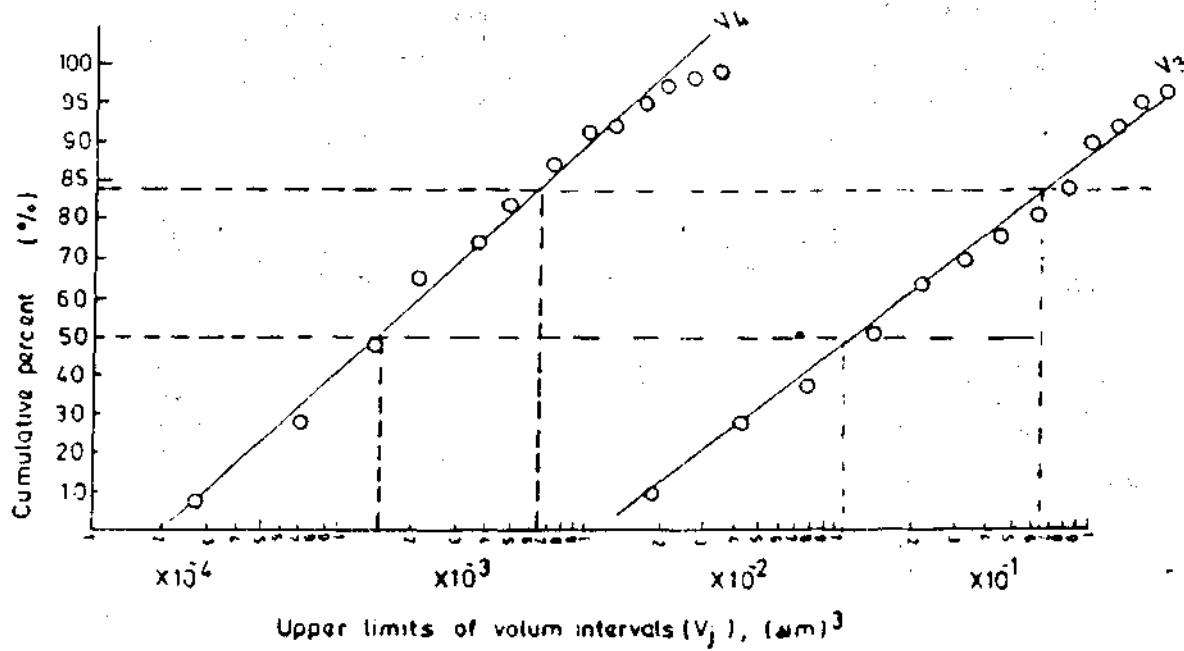


Fig.15b Volume cumulative curves for stage 3 and 4

Using equations 4.1.1 and 4.1.2 and 5.1.6 to 5.1.11, the values of the surface area and volume shape factors of the particles on each stage were evaluated and are shown in Table 5. Also the ratio D_p/D_s was calculated according to equation 4.1.3.

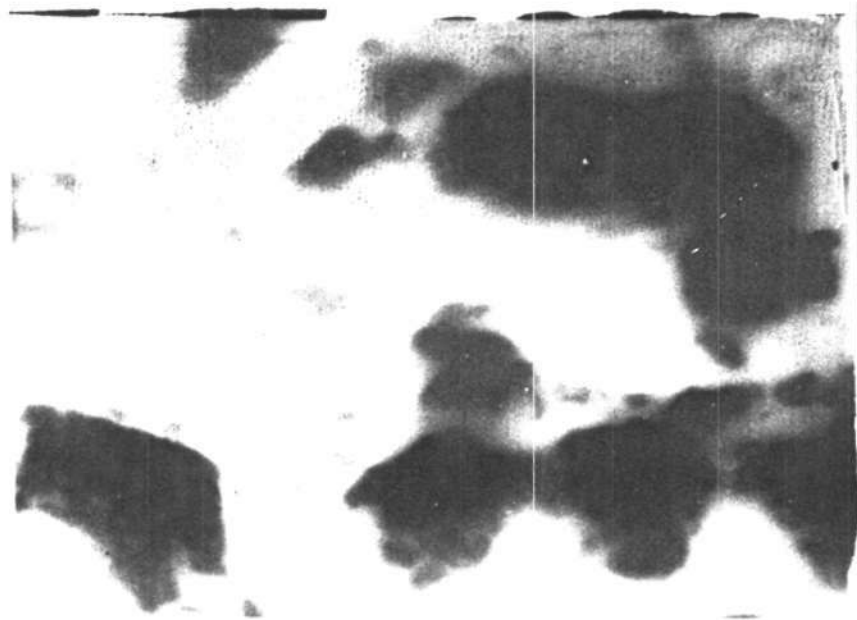
Table 5: Surface area and volume shape factors for each of the 4-stage of the Cascade Impactor

| P A R A M E T E R | S T A G E | | | | Average |
|---------------------------|-----------|-------|-------|-------|---------|
| | 1 | 2 | 3 | 4 | |
| Surface area shape factor | 3.28 | 3.13 | 2.79 | 3.18 | 3.1 |
| Volume shape factor | 0.49 | 0.49 | 0.41 | 0.55 | 0.49 |
| d_p/d_s | 1.045 | 1.033 | 1.097 | 1.779 | 1.23 |

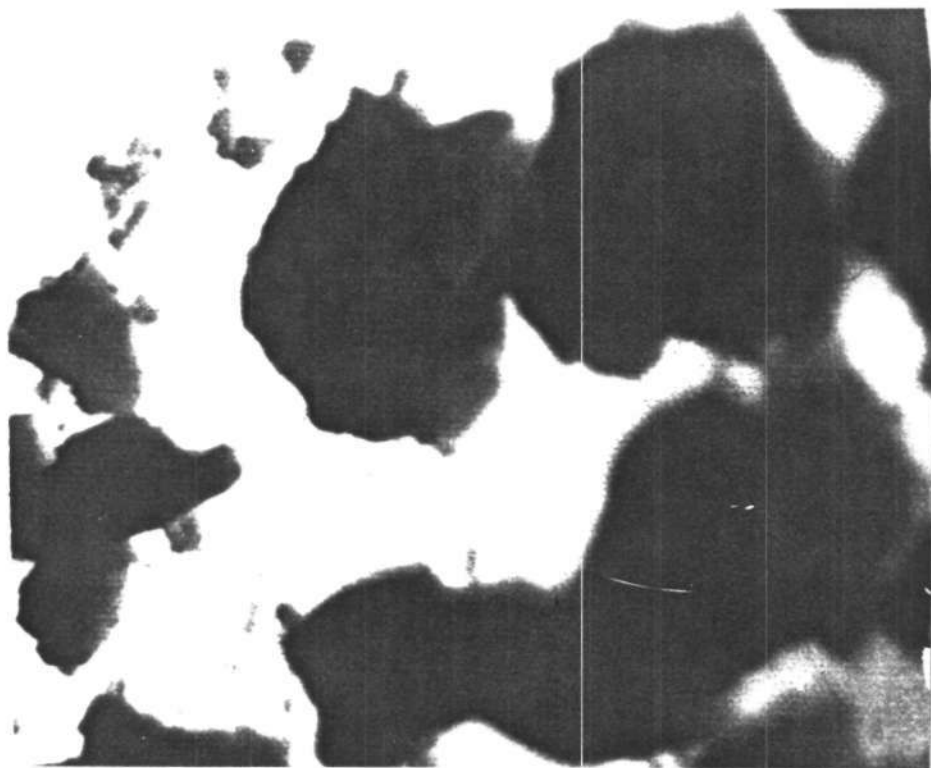
5.2 Transmission Electron Microscopy Results

After the specimen preparation described in Section 4.2.1 and following the procedure in the operating manual of Philips EM 400T, photomicrographs of the samples were obtained as shown in Figure 16. Micrographs were not obtained for stages 1 and 2 because the microscope could not give any illumination at magnifications lower than 2800 times (which is due to some fault in the instrument), and at this magnification only one or two particles of stage 1 and 2 can be in the field of view of the microscope. Since a large number of particles has to be counted for a dependable distribution, sizing of particles of stage 1 and 2 at this high magnification will definitely be a waste of the scarce photographic materials. Thus only the smaller sizes of stage 1 and 2 were sized and counted using TGZ 3 Counter.

Figure 16: Electron micrographs of the particles collected on stage 3 (a) and stage 4 (b).
(5600x)



a



b

A Plot of the percent cumulative of the particle diameters on a log-probability paper yield straight lines indicating a good fit to the log-normal distribution as shown in Figure 17. Though in this case deviations from straight lines were observed at larger diameter values just like the case of optical microscope measurements. The Rosin-Rammler equation was found to fit the data in this region as shown in Figure 11

Using equations 5.1.3 to 5.1.4 the mean diameters of the distribution on the two stages were calculated and the result shown in Table 6.

Table 6: Shows values of Mean diameter (\bar{D}) in microns using optical and Transmission electron microscope.

| MICROSCOPE | S T A G E | | | |
|---------------------|-----------|------|------|------|
| | 1 | 2 | 3 | 4 |
| Optical | 3.87 | 1.65 | 0.76 | 0.16 |
| Electron Microscope | - | - | 0.69 | 0.44 |

A comparison between optical and electron microscope counts of stage 3 and 4 was done by Chi-square test applied to the two methods, so as to find whether the results of the size distribution measurements depend on the type of microscope used.

The results are shown in Table 7. For stage 3 the Chi-square result for 14 degrees of freedom is 7.4 and is 9.1 for stage 4.

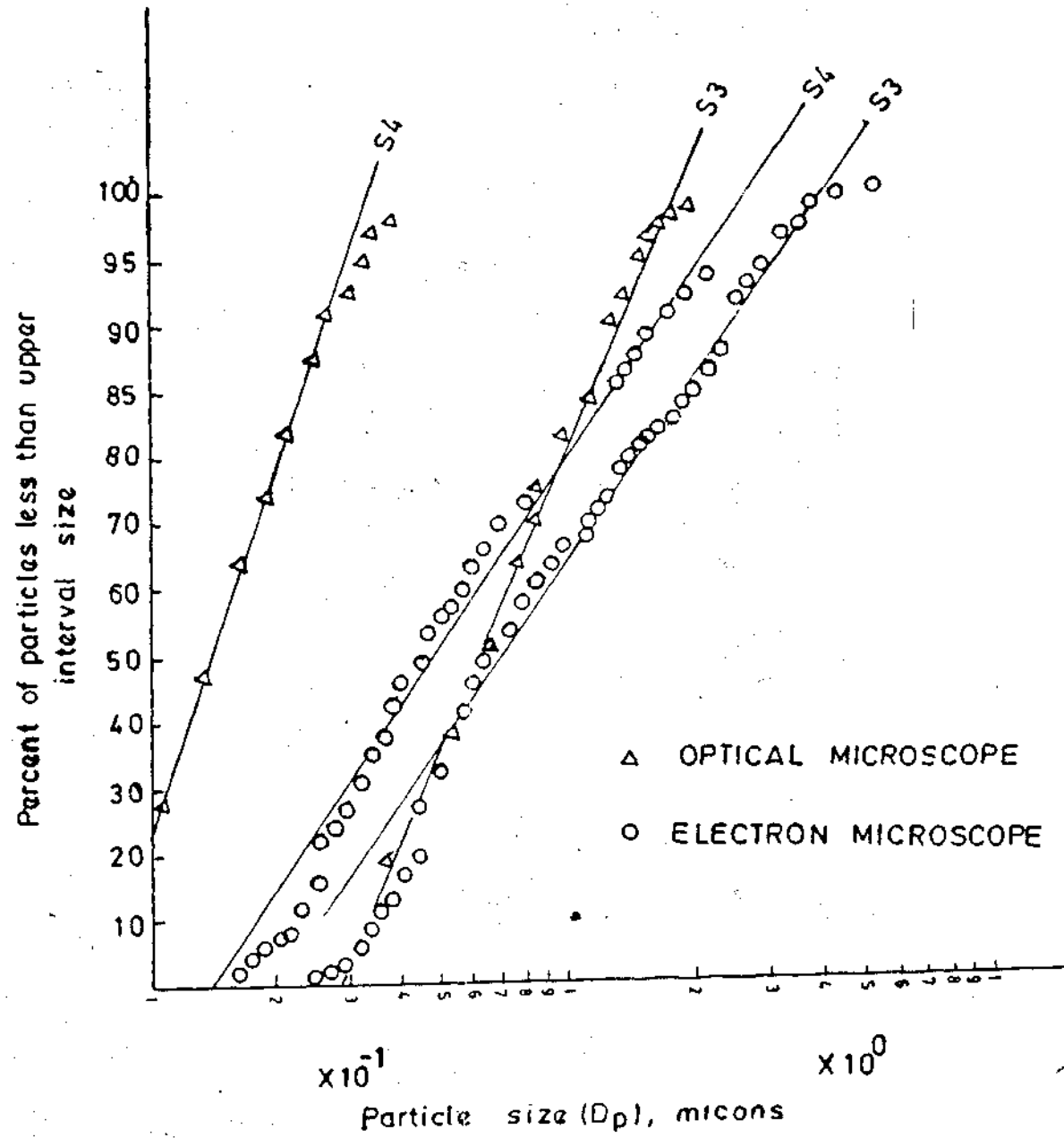


Figure 17: Cumulative curve for the particles using both optical and electron microscope

Table 7: Comparison between optical and electrom-microscope counts of stage 3 and 4

| Stage | Size Interval (μm) | Optical Counts | E.M. Counts | X^2 and degrees of freedom | Probability, P that differences b+w optical & E.M. |
|-------|---------------------------------|----------------|-------------|------------------------------|--|
| 3 | 0.23 - 0.33 | 43 | 43 | $X^2 = 7.4$ d.f = 14 | 0.05 > P |
| | 0.33 - 0.43 | 59 | 47 | | |
| | 0.43 - 0.53 | 55 | 35 | | |
| | 0.53 - 0.64 | 41 | 49 | | |
| | 0.64 - 0.74 | 38 | 28 | | |
| | 0.74 - 0.84 | 23 | 33 | | |
| | 0.84 - 0.94 | 22 | 10 | | |
| | 0.94 - 1.05 | 18 | 18 | | |
| | 0.05 - 1.15 | 13 | 23 | | |
| | 1.15 - 1.25 | 9 | 4 | | |
| | 1.25 - 1.35 | 6 | 13 | | |
| | 1.35 - 1.46 | 4 | 3 | | |
| | 1.46 - 1.56 | 4 | 2 | | |
| | 1.56 - 1.66 | 1 | 3 | | |
| | 1.66 - 1.77 | 1 | 1 | | |
| 4 | 0.14 - 0.16 | 65 | 74 | $X^2 = 9.1$ d.f = 14 | 0.05 > P |
| | 0.16 - 0.19 | 37 | 38 | | |
| | 0.19 - 0.21 | 67 | 77 | | |
| | 0.21 - 0.24 | 47 | 27 | | |
| | 0.24 - 0.27 | 79 | 71 | | |
| | 0.27 - 0.29 | 33 | 47 | | |
| | 0.29 - 0.32 | 9 | 26 | | |
| | 0.32 - 0.34 | 8 | 21 | | |
| | 0.34 - 0.37 | 14 | 10 | | |

Table 7 cont'd

| | | | | | |
|--|-------------|----|---|--|--|
| | 0.37 - 0.40 | 9 | 7 | | |
| | 0.40 - 0.42 | 6 | 6 | | |
| | 0. | | | | |
| | 0.42 - 0.45 | 10 | 1 | | |
| | 0.45 - 0.47 | 4 | 1 | | |
| | 0.47 - 0.51 | 5 | 1 | | |
| | 0.51 - 0.53 | 5 | 1 | | |

The comparison between optical and electron-microscope counts are shown in Table 7. Column four show the results of the Chi-square test for fourteen degrees of freedom. Column five show the probability that the difference in the two methods is due to chance alone. The full discussion of these surprising results is done in Section 6.1.

Chapter 6

DISCUSSION, CONCLUSION AND SUGGESTION FOR FURTHER WORK

6.1 DISCUSSION

The linear air speed (5.5 m/s) into the jet orifice of the sampler during sampling was greater than that of the approaching air stream (1.51 m/s). Therefore some particles because of their inertia fail to follow their air flow lines into the orifice causing the sizes of the particles to be under estimated or result in an-isokinetic sampling instead of the desired isokinesis. The correction factors for an-isokinesis were calculated from equations 2.1.1 to 2.2.2 and are shown in Table 1. The results show that anisokinesis effect is only significant in the case of the first stage where the size range is 1.44 - 10 μm . That of the other stages with size ranges less than 3 μm was found to be almost equal to one. The result is in good agreement with that obtained by May (1967). It was shown in his report that an-isokinesis effect is negligible for particles of diameter less than 5 μm .

The difference in the mineral composition of the dust from that obtained by Adetunji and Ong (1980) has clearly indicated that the Harmattan dust in the work reported here could emanate from different source regions, or from one source region having different rock strata. In a recent paper by Adetunji and Ong (1986), the variation was attributed to the geology of the source region; if the source rock strata have different mineral compositions, then erosion from

the source could result in seasonal variation in the dust composition. Also in undulating land surface, a variety of strata are likely to be exposed together, as depicted in Figure 18, where minerals from the different strata (A, B and C) combine to form the dust collected at a particular season.

The results of the X-ray diffraction analysis show that quartz is the major constituent of the Harmattan dust, with small concentration of other clay minerals. The existence of microcline ($KAlSi_3O_8$) on all the four stages hitherto unreported, is rather interesting. Since feldspars unlike quartz are usually regarded as unstable when fine grained. They are usually found in sand size grains. Their existence in microsized is most probably associated with abrasion in the desert area of virtually unweathered rocks. It is unlikely, therefore that they are produced from chemically weathered rocks as suggested by Junge (1979). This is because any chemical weathering of the feldspar grains must have been further inhibited by the very dry nature of the transporting Harmattan winds. Also it was reported by Gillette and Walker (1977) that abrasion of limestone, feldspar and quartz increases with grain size, wind velocity and surface roughness.

The height of the X-ray diffraction peaks reduces from stage one to four. This shows a direct dependence of the height of diffraction peak with particle size range.

Log-normal distribution was chosen in this work because, as reported by Gillette and Walker (1977), it was found

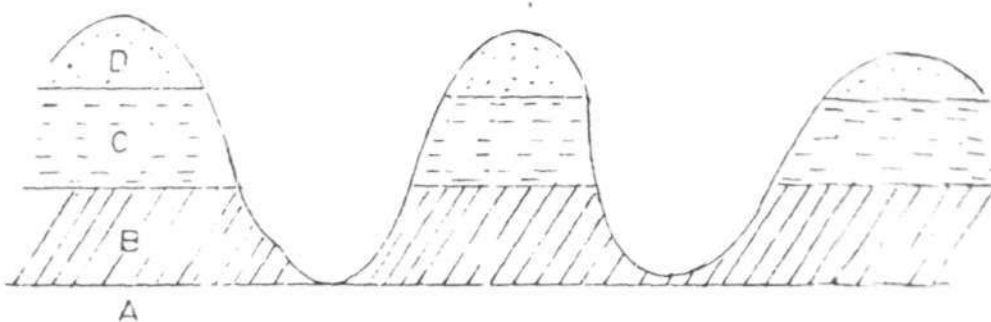


Figure 18: Undulating land surface showing variety of strata, (A, B, C and D) exposed. (From Adetunji and Ong, 1986).

empirically to fit the soil-derived aerosols well. Furthermore, because of the nature of formation of the Harmattan dust particles that is by communitive processes which was described by Epstein (1947), give rise to a log-normal distribution. Lastly because it is mathematically less complex, and its relative ease in evaluating particulate parameters

The skewness observed in Figure 8 shows that the dust is not normally distributed and this led to the choice of another distribution. Plots in Figure 9 and 10 show that a single log-normal distribution fit the data well, though with slight modification at higher diameter values, Rosin-Rammler equation was found to fit well.

Evaluation of the measures of central tendency yields 2.33, 1.03 μm and 0.35 μm as values of σ_g , \bar{D} and D_m respectively. The value of mean diameter (\bar{D}) obtained is of special interest if one considers it in terms of scattering efficiency of aerosols. In his report, Friedlander (1977), maintained that the particles within the range of 0.1 to 1.3 μm diameter have the highest scattering efficiency of the solar radiation. This could be responsible for the great reduction in visibility during peak periods as recorded in Table 2. Also, the fraction of harmattan dust particles deposited in the lungs of individuals is expected to be low since according to Friedlander's report, particles in the size range of 0.1 to 1 μm are too large to diffuse rapidly onto the lungs and too small to settle rapidly or deposit because of inertial effects. Though deposition is also

expected to vary from individual to individual depending on lung geometry and air flow patterns..

The mean diameters obtained for each stage using semi-automatic counter differ significantly from those obtained using Porton graticule sizer. This implies that the distribution measurements depends on the types of counter used. However, more errors are likely to be associated with Porton graticule counting and sizing since repeated counting cannot be completely eliminated in this case. Also the circles in Porton graticule are not adjustable for proper sizing of the particles as is obtained in the electronic counter.

Results of the comparison between optical and Electron microscope counts show that the two methods are independent. This is rather unexpected since the difference in resolution of the two microscopes is expected to yield results that differ significantly. A possible explanation for the observed result is that some particles must have been lost during sample preparation for electron microscope.

The variation of shape factors with size range reported by Robins (1954) is also observed in the Harmattan dust. The values of both surface area and volume shape factors of the analysed samples show a general decrease from stage one to three, except at stage four where the values increases; this could be associated with an inherent leakage at the third stage. The value of the ratio D_p/D_s found to be 1.24 is closer to a value of 1.33 obtained by Watson (1953) for coal dust.

6.2 Conclusion and Suggestion for further Work

The X-ray diffraction results suggest the possibility of variable source regions when compared with other previous results. Alternatively, the source could be the same region but with rock strata having different mineral composition. In this case the periodic erosion of different mineral types could be transported from time to time. The variation of mineral composition with the size range could be explained as follows: the dust particles are formed by preferential breakage of certain minerals into a given size range.

In addition the results in this work have shown that quartz is the single major constituent of the Harmattan dust.

The log-normal distribution was found to fit the data well, except for some deviation at larger diameter values. But Rosin-Rammler equation fits this region well. The mode and mean diameter values obtained show that Harmattan dust contribute significantly in the scattering of radiation from the sun, which is responsible for the observed reduction in visibility. Also, continued deposition of the Harmattan dust over long periods might have an adverse toxic effect on humans and other animals exposed to this unique natural atmospheric aerosol.

Comparison of the results obtained with semi-automatic counter and Porton graticule show that the distribution is dependent on the instrument used for sizing and counting. But, comparison between electron and optical microscopes counts show that the results are independent of the type of microscope used.

Very little has been studied about the harmattan dust transported over the area of this study. However, a lot has been done on the forecasting of it. The results obtained here and in other works suggest that the mechanism of dust production is complex. Therefore, emphasis should be laid on finding the mechanics of Harmattan dust formation, suspension, transportation and deposition, since it is through one of these processes that the dust affect us or our ecology. The non-availability of certain items of equipment has limited the scope of investigation of the harmattan dust. For a complete characterization of the harmattan dust, however, the following investigations need to be carried out to augment the tremendous efforts made so far.

They include:

- (1) The relationship between particle size or concentration with optical constants, health effects and other ecological effects need to be fully investigated.
- (2) The variation of chemical composition of the dust as it is transported along the route should be studied so as to determine the mineral input into our sub-soil.
- (3) The radio-activity of the Harmattan dust, since the trade winds are likely to carry dust from uranium rich areas in Niger Republic.

Finally, it is highly recommended that all efforts should be geared towards forming an enlarged group which embraces other disciplines to forecast, track and fully characterize this unique aerosol which is everyday gaining global a-tention. Cooperation with concerned meteorological

centres should ease the problem of meteorological data collection and evaluation.

REFERENCES

- Adefolalu, D.O. (1968). Two Case-Studies of the vertical distribution of dust during occurrence of Harmattan haze over Nigeria. Technical Note, 21, Meteorological Department, Lagos, Nigeria, 13 - 18.
- Adetunji, J., McGregor, J. and Ong, C.K. (1974). The Harmattan haze. Weather J1, 34, 430 - 436
- Adetunji, J. and Ong, C.K., (1980). Qualitative analysis of the Harmattan haze by X-ray diffraction. Atmospheric Environment, 14, 857 - 858.
- Adetunji, J. and Ong, C.K. (1986). Variation of Elemental Composition of the Harmattan dust. Atmospheric Environment (submitted).
- Aina, J.O. (1972). A contribution to the forecasting of Harmattan dust haze. Quarterly Meteorological Magazine, 2 Journal of Nigerian Meteorological Service, 12, 77 - 89.
- Alexander, L., Klug, H.P. and Kummer, E. (1948). Statistical factors affecting the Intensities of X-rays diffracted by Crystalline Powders. Journal of Applied Physics, 19, 742 - 753.
- Bradley, D.E. (1967). The preparation of Specimen support film. In : Desmond, K. (Ed.) Techniques for Electron microscopy - Blackwell Scientific Publications Limited, Oxford, pp. 58 - 74
- Calson, T.N. and Prospero, J.M. (1972). Vertical and areal distribution of Saharan dust over the Western equatorial

- North Atlantic ocean. Journal of Geophysical Research,
77, 5255 - 5265.
- Carl Zeiss TGZ-3 Particle Counter and Sizer. Operating
Instructions.
- Cartwright, J. (1954). The electron Microscopy of airborne
dusts. British Journal of Applied Physics, Suppl.
No. 3, 109 - 120.
- Davies, C.N. (1968). The entry of aerosols into sampling
tubes and heads, British Journal of Applied Physics,
Nos. 2 1 921 - 926.
- Davies, C.N. (1974). Size distribution of Atmospheric
particles. Journal of Aerosol Science, 5, 293 - 300.
- Davies, C.N. (1976). The Mathematical Expression of the
size distribution of Atmospheric aerosols. Journal
of Aerosol Science, 7, 255 - 259.
- Davies, C.N. (1979). Fluid-Particle interaction. Journal
of Aerosol Science, 10, 477 - 513
- De Wolf, P.M., Taylor, J.M. and Parrish, W. (1959). Effects
of Crystallite Size on X-ray Intensities. Journal of
Applied Physics, 30, 63 - 69
- Epestein, B. (1947). The Mathematical description of Certain
breakage mechanisms leading to the logarithmico -
normal distribution. Journal of Franklin Institute,
244, 471 - 477.

- Friedlander, S.K. (1960). Similarity Considerations for the particle size spectrum of a coagulating, sedimenting aerosol. Journal of Meteorology, 17: 479 - 483.
- Friedlander, S.K. (1961). Theoretical consideration for the particle size spectrum of the Stratospheric aerosol. Journal of Meteorology, 18: 753 - 759
- Friedlander, S.K. (1977). Fundamentals of Aerosol behavior. John Wiley and Sons., New York, pp. 1 - 23
- Fuchs, N.A. (1975). Sampling of aerosols. Atmospheric Environment, 9: 697 - 700
- Gillette, D.A. and Walker, T.R. (1977). Characteristics of airborne particles produced by Wind erosion of sandy soil of High plains of West Texas. Soil Science 123(2): 97 - 110
- Gillette, D.A. (1979). Environmental factors affecting dust emissions by wind erosion. In: Morales C. (Ed.) Saharan Dust Scope 14 - John Wiley and Sons, New York, pp. 71 - 89
- Grundy, P.J. and Jones, G.A. (1976). In Coles, R.R. (Ed.) Electron microscopy in the study of materials, The structure and properties of Solids. 7 - Edward Arnold, London, pp. 1 - 25
- Hamilton, R.A. and Archbold, J.W. (1945). Meteorology of Nigeria and adjacent territory. Quarterly Journal of Royal Meteorological Society. 71: 231 - 265

- Junge, C.E. (1955). The size distribution and aging of natural aerosols as determined from electrical and optical data on the atmosphere. Journal of Meteorology, 12: 13 - 25
- Junge, C.E. (1969). Comments on Concentration and Size distribution measurements of Atmospheric aerosols and Test of the Theory of Self-preserving size distribution. Journal of the Atmospheric Sciences, 26: 603 - 608.
- Junge, C.E. (1979). The importance of Mineral dust as an Atmospheric constituent. In : Morales, C. (Ed.) Saharan Dust Scope 14 - John Wiley and Sons, New York, pp. 41 - 60
- Kalu, A.E. (1979). The African dust plume: Its characteristics and Propagation across West Africa in Winter. In : Morales, C. (Ed.) Saharan Dust, Scope 14 - John Wiley and Sons, New York, pp. 95 - 118.
- Kotrappa, P. (1972)). Shape factors for aerosols of Coal, UO_2 and ThO_2 in respirable size range. In : Mercer, T.T., Morrow, P.E. and Stober, W. (Eds.) Assessment of Airborne Particles - Charles, C. Thomas, Springfield Illinois, pp. 5 - 15.
- Lundholm, B. (1979). Ecology and dust transport. In : Morales, C. (Ed.) Saharan Dust. Scope 14 - John Wiley and Sons, New York, pp. 61 - 68

- May, K.R. (1967). Physical aspects of sampling airborne microbes. In : Gregory, P.H., Montheith, J.L. (Eds.) Airborne Microbes - Cambridge University Press, London.
- Orr, C. and Dallavalle, J.M. (1959). Fine Particle Measurement - Size, Surface and Pore Volume. The McMillan Company, New York, pp. 13 - 42
- Paceri, R.E. and Friedlander, S.K. (1965). Measurements of Particle Size distribution of the Atmospheric aerosol. Journal of the Atmospheric Science. 22: 577 - 584
- Patterson, E.M., Gillette, D.A., and Grams, G.W. (1976). The relation between Visibility and the Size-number distribution of airborne soil particles. Journal of Applied Meteorology. 15, 470 - 478
- Patterson, E.M. and Gillette, D.A. (1977). Commonalities in measured size distribution for aerosols having a Soil-derived Component. Journal of Geophysical Research 82: 2074 - 2082
- Patterson, E.M. and Gillette, D.A. (1977). Measurements of Visibility versus mass-concentration for air-borne soil particles. Atmospheric Environment, 11: 19 11: 193 - 196
- Peterson, C.M. (1972). Aerosol Sampling for Particle Size analysis. Air Sampling Instruments. American Conference of Governmental Industrial Hygienists.
- Powder Diffraction File Search Manual for Minerals (1974). First Ed. Joint Committee on Powder diffraction

Powder Diffraction File Search Manual for Minerals (1974).

First Ed., Joint Committee on Powder diffraction
Standards, Philadelphia.

Prospero, J.M. (1968). Atmospheric dust studies on Barbados.

(Bull. American Meteorological Society, 645 - 652

Prospero, J.M. and Carlson, T.M. (1979). Radon-222 in the

North Atlantic trade winds. Its relationship to dust
transport from Africa. Science, 167: 974 - 977.

Robins, W.H.M. (1954). The Significance and Application of

shape factors in Particle size analysis. British
Journal of Applied Physics. Supplement No.3: 82 - 85.

Robins,, -. (1976). Wind over Africa. Geography Magazine,

48: 218 - 220.

Selected Powder Diffraction Data for Minerals (1974). First

Ed., Joint Committee on Powder diffraction standards.
Philadelphia.

Schutz, L. and Jacnicke, R. (1974). Particle number and

mass distribution above 10^{-4} cm radius, in sand and
aerosols of the sahara desert. Journal of Applied
Meteorology, 13: 863 - 970

Technical Reports No.179 (1978). Particle Size Analysis

in estimating the Significance of Airborne Contamina-
tion. International Atomic Energy Agency, Vienna,
205 - 229.

Vassamillet, I.F. and King, H.W. (1967). Diffractometer techniques. In : Kaelble, E.F., (Ed.) - Handbook of X-rays - McGraw Hill Book Company, New York

William, E.C. and Whitby, K.T. (1967). Concentration and size distribution measurements of Atmospheric aerosols and a test of the theory of self-preserving size distribution. Journal of the Atmospheric Sciences, 24: 677 - 686

Wilson, I.G. (1971). Desert Sandflow basins and a model for the development of ergs. Geography Journal, 137: 180 - 198

Yaalon, D.H. and Ganor, E. (1979) East Mediterranean Trajectories of Dust carrying storms from the Sahara and Sinai. In : Morales, C. (Ed.) Saharan Dust Scope 14 - John Wiley and Sons, New York, pp. 187 - 193

Zebel, G. (1978). Some problems in sampling of aerosols. In: David, T.S. (Ed.) Recent development in Aerosol Science - John Wiley and Sons, New York, pp. 167 - 185

APPENDIX A

MATHEMATICAL EXPRESSION OF THE LOG-NORMAL DISTRIBUTION

$$\frac{dN}{d \ln D} = \frac{N}{\ln \sigma_g \sqrt{2\pi}} \cdot \exp \left[-\frac{1}{2} \left(\frac{\ln D - \ln D_0}{\ln \sigma_g} \right)^2 \right] \quad \text{A.1}$$

dN is the number of particles in the size range between D and $D + dD$.

N = total number of particles

$$\text{Since } \int_0^{\infty} \frac{1}{N} \frac{dN}{d \ln D} \cdot d \ln D = 1.$$

$$\therefore \bar{D} = \int_0^{\infty} D \cdot \frac{1}{N} \cdot \frac{dN}{d \ln D} \cdot d \ln D \quad \text{A.2}$$

$$\bar{D} = \int_0^{\infty} \frac{ND}{\ln \sigma_g \sqrt{2\pi} N} \cdot \exp \left[-\frac{1}{2} \left(\frac{\ln D/D_0}{\ln \sigma_g} \right)^2 \right] \cdot d \ln D \quad \text{A.3}$$

$$\text{putting } z = \frac{\ln D/D_0}{\sqrt{2 \ln \sigma_g}}$$

$$d \ln D = \sqrt{2 \ln \sigma_g} dz$$

$$\bar{D} = \frac{1}{\sqrt{2\pi} \cdot \ln \sigma_g} \int_{-\infty}^{\infty} D \exp \left[-\frac{(\ln D - \ln D_0, g)^2}{2 \ln^2 \sigma_g} \right] \cdot \sqrt{2 \ln \sigma_g} dz \quad \text{A.4}$$

$$\bar{D} = \frac{1}{\sqrt{2\pi} \cdot \ln \sigma_g} \int_{-\infty}^{\infty} D \exp \left[-z^2 \right] \cdot \sqrt{2 \ln \sigma_g} dz \quad \text{A.5}$$

$$D = D_0, g \exp (z \sqrt{2 \ln \sigma_g})$$

$$\bar{D} = \frac{1}{\sqrt{\pi}} \int_{-\infty}^{\infty} D_{o,g} \exp(-z^2 + \sqrt{2} \ln \sigma_g z) dz \quad \text{A.6}$$

$$\text{put } y = z - \frac{\ln \sigma_g}{\sqrt{2}}$$

$$\bar{D} = \frac{D_{o,g}}{\sqrt{\pi}} \int_{-\infty}^{\infty} \exp\left(-y^2 + \frac{\ln^2 \sigma_g}{2}\right) dy \quad \text{A.7}$$

$$\text{Using } \int_{-\infty}^{\infty} \exp(-y^2) dy = \sqrt{\pi} \quad \text{or} \quad \int_0^{\infty} \exp(-y^2) dy = \frac{\sqrt{\pi}}{2}$$

$$\Rightarrow \bar{D} = D_{o,g} \exp\left(\frac{1}{2} \ln^2 \sigma_g\right) \cdot \frac{1}{\sqrt{\pi}} \int_{-\infty}^{\infty} \exp(-y^2) dy \quad \text{A.8}$$

$$\bar{D} = D_{o,g} \exp\left(\frac{1}{2} \ln^2 \sigma_g\right) \quad \text{A.9}$$

$$\bar{D} = \exp(\ln D_{o,g} + \frac{1}{2} \ln^2 \sigma_g) \quad \text{A.10}$$

Also

$$\bar{D}^2 = \exp(2 \ln D_{o,g} + 2 \ln^2 \sigma_g) \quad \text{A.11}$$

$$\bar{D}^3 = \exp(3 \ln D_{o,g} + \frac{9}{2} \ln^2 \sigma_g) \quad \text{A.12}$$